430 *Chem. Mater.* **2011,** *23,* 430–445
DOI:10.1021/cm102166j

CHEMISTRY OF MATERIALS
Review

Systematic Nanoengineering of Soft Matter Organic Electro-optic Materials†

Larry R. Dalton,*,‡ Stephanie J. Benight,‡ Lewis E. Johnson,‡ Daniel B Knorr, Jr.,§ Ilya Kosilkin,‡ Bruce E. Eichinger,‡ Bruce H. Robinson,‡ Alex K.-Y. Jen,⊥ and René M. Overney§

‡*Department of Chemistry, University of Washington, Seattle, Washington 98195-1700, United States,* §*Department of Chemical Engineering, University of Washington, Seattle, Washington 98195-1750, United States, and* ⊥*Department of Materials Science & Engineering, University of Washington, Seattle, Washington 98195-2120, United States*

Received August 1, 2010. Revised Manuscript Received September 28, 2010

An overview of the development and utilization of organic electro-optic materials is presented with emphasis on the role played by quantum and statistical mechanical calculations in understanding critical structure/function relationships that have guided the improvement of such materials over the past two decades. This review concentrates largely on three classes of organic electro-optic materials prepared by electric field poling of materials near their glass transition temperature: (1) chromophore/polymer composite materials, (2) dendrimers and polymers containing covalently incorporated chromophores, and (3) matrix-assisted-poling (MAP) materials where specific spatially anisotropic interactions enhance poling efficiency. In particular, the role of chromophore shape, restrictions on chromophore motion associated with covalent bonds, and lattice dimensionality effects are reviewed. The role of device design and auxiliary properties (optical loss, thermal stability, photochemical stability, processability) in influencing the utilization of organic electro-optic materials is also briefly reviewed.

Introduction

Organic nonlinear optical (ONLO) materials have always afforded the possibility of ultrafast response to time-dependent applied electric fields. The phase relaxation times of extended conjugation π-electron systems are typically on the order of tens of femtoseconds,[1] which translate to the possibility of device bandwidths of tens of terahertz.[2,3] The potential for increased bandwidth performance was a strong motivation for early (late 1980s and early 1990s) research efforts. This motivation diminished in the 1990s with the introduction of wavelength division multiplexing (WDM) and code division multiplexing (CDM) techniques, which have significantly reduced bandwidth demands placed on direct time division multiplexing (TDM). However, bandwidth demands of telecommunications and computing have continued to grow and particularly with increased demand for high-density video information, e.g., video conferencing, combined delivery of television and Internet services, defense demands for real time sensing and imaging, etc.

Another strong motivation for research on ONLO materials is the potential for exceptionally large optical nonlinearities, specifically for optical nonlinearities exceeding those of inorganic semiconductor and crystalline materials. Seemingly endless possibilities exist for structural modification of organic materials to increase optical nonlinearity, providing a strong motivation for the design and synthesis of new materials. The focus of this review is to cover theoretical methods that have contributed to the improvement of the optical nonlinearity of organic electro-optic materials through definition of important structure/function relationships. We review past efforts as well as provide insights into how much organic electro-optic activity can be improved in the future.

Response time and optical nonlinearity are not the only performance parameters required of organic materials to be successful in device applications. Optical loss, thermal stability, and photostability are all very important. Although these issues are a minor focus in this review, substantial progress has been made in improving these performance parameters. This research has been covered in other reviews (and references cited therein including to even earlier reviews).[4−14] Another factor which has recently impacted the commercial viability of ONLO materials is the advance in device engineering, particularly the advent of silicon photonics.[10−12,15−20] The high index of refraction of silicon has permitted a dramatic reduction in the size of photonic circuitry. As a result, this circuitry is more size compatible with very large scale integration (VLSI) electronic circuitry in chipscale integration of photonics and electronics. More recently, the integration of organic electro-optic (OEO) materials into slots (as small

† Accepted as part of the "Special Issue on π-Functional Materials".
*Corresponding author. E-mail: dalton@chem.washington.edu. Tel.: (206) 543-4020. Fax: (206) 685-8665.

 Published on Web 11/08/2010

as 25 nm) in silicon photonic waveguides has permitted dramatic enhancement of the performance of organic electro-optic materials through concentration of optical fields and reduction of electrode separation (used to apply radiofrequency fields). For example, drive voltages required for transducing electrical and optical information and for optical switching have been reduced to 0.25 V using slotted silicon device structures even with organic electro-optic materials of modest activity.[17] In traditional (all organic) device structures, OEO materials exhibiting an order of magnitude greater electro-optic activity are required to achieve similar drive voltages.[10,21] An even greater enhancement in the performance of OEO materials may be possible with slotted waveguide device structures where both radiofrequency and optical fields are enhanced by concentration into a nanoscopic slot.[22] While organic electro-optic materials have not been significantly studied as components of plasmonic device structures, plasmonic devices[23] are beginning to show promising performance when fabricated from inorganic materials; use of organic electro-optic materials seems to be a logical extension.

This review concentrates on ONLO materials prepared by electric field poling of thin film materials (which have been deposited on appropriate substrates by spin-casting) near the glass-transition temperature of the macromolecular material. We will concentrate on dipolar electro-optic chromophores, although octupolar chromophores have also been studied (see the Conclusions and Future Prospects section). ONLO materials can also be prepared by crystal growth and by sequential synthesis/self-assembly methods (see the Conclusions and Future Prospects section), but these will not be reviewed here.

Before launching into a more detailed discussion of theory and experimental results, we will first introduce some basic concepts and terminology that will make the subsequent discussion and cited literature more comprehensible. Electrically-poled dipolar or charge-transfer chromophores exhibit two nonzero electro-optic tensor elements (r_{33} and r_{13}) with values expressed in picometers (pm) per volt (V), i.e., the phase shift of light produced by application of a given voltage. Typically, $r_{33} \geq 3r_{13}$, with the exact value depending on the extent of acentric order induced by the electric poling field. In the low order limit (and neglecting the minor elements of the molecular first hyperpolarizability tensor), $r_{33} = 3r_{13}$. Because r_{33} is the largest value, device engineers typically attempt to utilize this value. This principal element of the electro-optic tensor represents macroscopic (material) electro-optic (EO) activity and is approximately related to the molecular first hyperpolarizability of the organic electro-optic (OEO) chromophore by the following expression

$$r_{33} = 2N\beta_{zzz}(\omega,\varepsilon)\langle\cos^3\theta\rangle\left\{\frac{g(\omega)}{{n_\omega}^4}\right\} \qquad (1)$$

where N is the chromophore number density (chromophores per cubic centimeter), $\beta_{zzz}(\omega,\varepsilon)$ is the principal element of chromophore (molecular) first hyperpolarizability tensor, $\langle\cos^3\theta\rangle$ is the acentric (or noncentrosymmetric) order parameter, $g(\omega)$ is a local field term representing the medium of finite dielectric permittivity, and n_ω is the index of refraction at the optical frequency of interest.

In early research, each of these parameters was assumed to be independent of the others. With this assumption, optimizing electro-optic activity, r_{33}, was considered a problem of using quantum mechanics to optimize β and using statistical mechanics to optimize $\langle\cos^3\theta\rangle$. For example, in the limiting case of noninteracting chromophores, acentric order is easily shown to be approximately given by

$$\langle\cos^3\theta\rangle = L_3\left(\frac{\mu g(0)F(0)}{kT}\right) \approx \frac{\mu g(0)F(0)}{5kT} \qquad (2)$$

where L is the Langevin function, μ is the chromophore dipole moment, $F(0)$ is the applied (dc) poling field, $g(0)$ is the dc local field factor, k is the Boltzmann constant and T is the Kelvin poling temperature. This simple form assumes that the chromophore can undergo reorientation (rotation) in three dimensions under the influence of the applied poling field. However, because of the presence of strong chromophore dipole−dipole interactions, the parameters of (eq 1) are not independent of each other. There are two components to the dipole−dipole interaction; one component favors centrosymmetric (centric) order, whereas the other favors noncentrosymmetric (acentric) order. Repulsive (steric) interactions also influence the movement of chromophores under the action of the poling field and influence the relative contributions that the two components of chromophore dipolar interaction make to $\langle\cos^3\theta\rangle$.

For chromophore−polymer composite materials, chromophores interact only very weakly with the polymer matrix. Therefore, consideration of the competition of chromophore electronic dipolar interactions and nuclear repulsive interactions are sufficient to understand $N\langle\cos^3\theta\rangle$, i.e., the loading parameter: the dependence of acentric order on chromophore number density.[24] For chromophores with strong dipolar interactions (large dipole moments), electro-optic activity is observed to go through a maximum with increasing chromophore number density. The maximum shifts to lower number density with increasing chromophore dipole moment (a μ^2 dependence is observed).

Chromophores incorporated physically into polymer hosts to form composite materials are not the only type of organic electro-optic (OEO) material prepared. For example, chromophores can be covalently incorporated into polymer, dendrimer, and dendronized polymer materials.[25−28] For these materials, the restrictions on chromophore motion associated with covalent bond potentials must be taken into account in order to understand poling-induced acentric order. Chromophores in most chromophore/polymer composite materials and in most macromolecular materials containing covalently incorporated chromophores undergo approximately 3D motion in the presence of the poling field. More specifically, effective 3D motion can occur because the chromophore molecules are undergoing reorientation independent of the surrounding polymer (macromolecular) host. Effective 3D motion can also result in the case where chromophore

motion is tightly coupled to the motion of the surrounding macromolecular (polymer/dendrimer) host if the correlation (persistence) length for motion of that host is short, so that both guest and host reorient together.

Recently, a third class of OEO materials has been introduced: matrix-assisted-poling (MAP) materials, where specific spatially anisotropic interactions enhance poling efficiency. For these materials, the effective lattice dimensionality surrounding the EO chromophore is less than 3D; thus, restricting the motion of the chromophore in the presence of the poling field. As shown in Figure 1, reducing lattice symmetry can enhance acentric order and thus electro-optic activity.

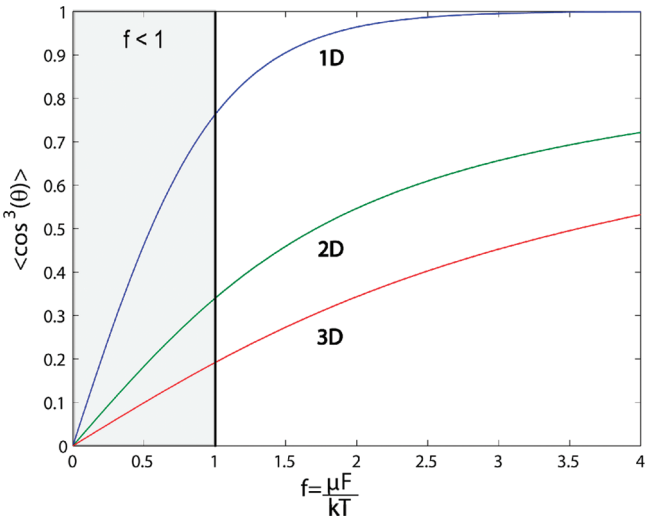

Figure 1. Acentric order is shown as a function of normalized poling energy, $f = \frac{\mu g(0) F(0)}{kT}$, where μ is the dipole moment, $F(0)$ is the applied poling field, $g(0)$ is the Onsager local field factor, k is the Boltzmann constant, and T is the Kelvin poling temperature. For the material systems discussed herein, the plots in the low field limit range (highlighted) are the most relevant.

The phenomenon of matrix assisted poling arises in materials where specific spatially anisotropic intermolecular interactions introduce a finite correlation length for "lattice" reorganization. Various restrictions imposed on EO chromophores loosely categorize the lattice dimensionality into three trends of order: (1) a molecule that exhibits "3D" type order has little to no dimensional restriction imposed upon it; (2) a molecule that exhibits "2D" order is restricted to orientation within a plane; and (3) a molecule with "1D" order can only point up or down along its internal unique axis. Specific MAP interactions include coumarin-coumarin interactions,[26,30] arene-perfluoroarene interactions,[10,28,29,31] and optically poled host materials (e.g., the DR1-co-PMMA host)[32] (see Figure 2 for examples of each of these). Binary chromophore organic glasses (BCOGs)[10,12,13,29,33] consisting of a chromophore guest doped into a chromophore-containing host also represent an example of MAP materials.

In this review, we will focus largely on MAP materials including how dimensionality is measured and the effect of dimensionality on electro-optic activity. Furthermore, we will explain in detail how lattice dimensionality can be

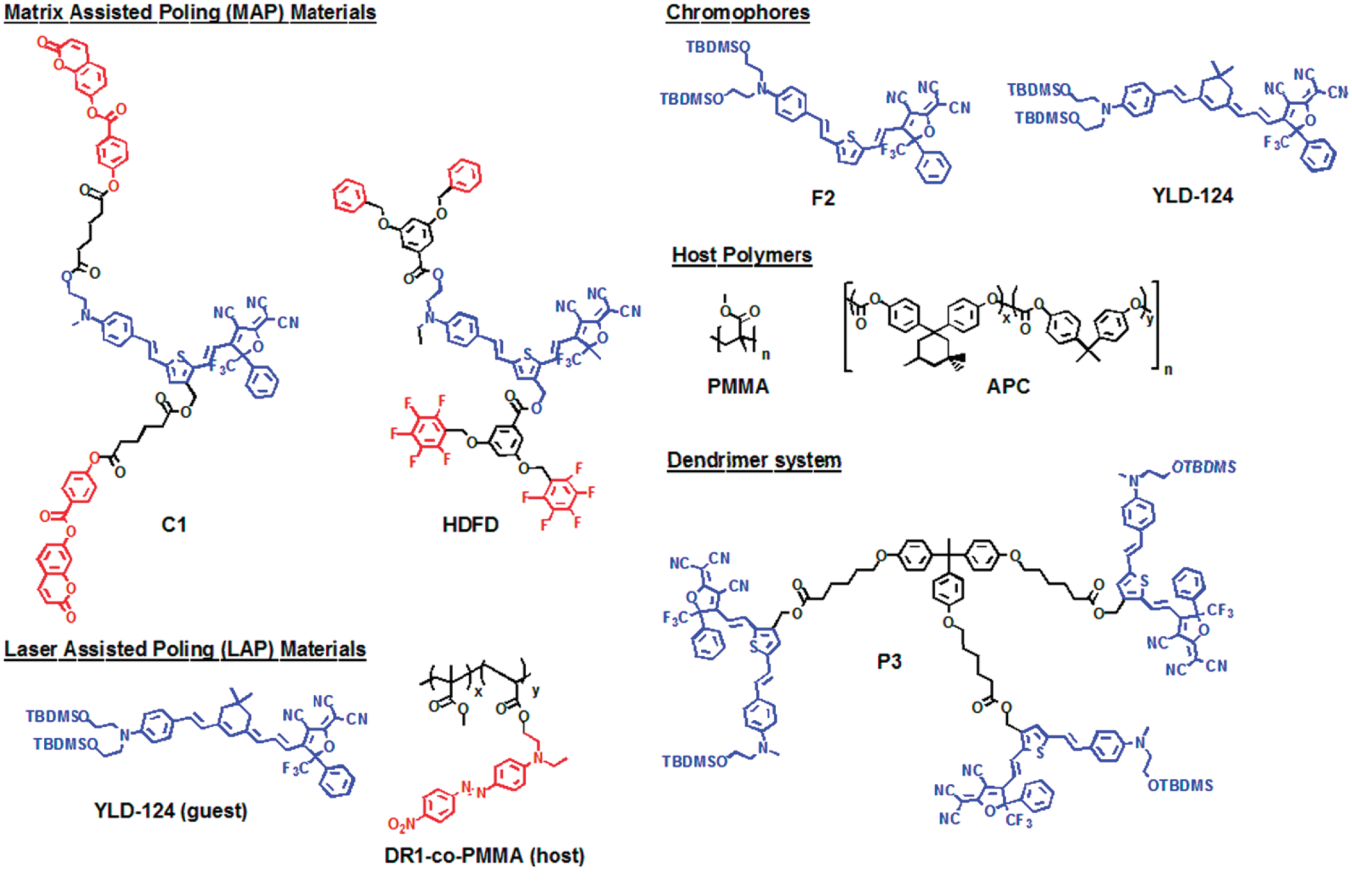

Figure 2. Matrix-assisted poling (MAP) materials (left). Other materials discussed in this review (right).

defined by measuring the relation between the acentric order parameter $\langle\cos^3\theta\rangle$ and the centrosymmetric order parameter, $\langle P_2\rangle$, which is related to the second order parameter with respect to the poling axis through

$$\langle P_2\rangle = \frac{3\langle\cos^2\theta\rangle - 1}{2} \quad (3)$$

Statistical mechanics calculations and dimensionality concepts illustrate how electro-optic activity can be optimized by controlling chromophore shape and the lattice environment that surrounds the chromophore. Quantum mechanical calculations are also required for optimization of chromophore hyperpolarizability β_{zzz}. We briefly review various quantum mechanical approaches and in particular, we will consider the effect of optical frequency (ω) and dielectric permittivity (ε) on molecular first hyperpolarizability. Taken together, both quantum and statistical mechanics permit a quantitative understanding of the contribution of the variables on the right side of (eq 1) to macroscopic electro-optic activity.

After providing an overview of quantum and statistical mechanical methods, we will conclude this review by mentioning characterization methodologies that have facilitated testing of theoretical concepts. Finally, we will conclude with a brief discussion of other considerations, which have impacted the practical use and commercialization of organic electro-optic materials.

Quantum Mechanics and Molecular Hyperpolarizability

Phenomenology. The interaction between matter and electromagnetic fields is described at the macroscopic level by Maxwell's equations.[34] For our purposes, only one constitutive equation is required: $D = \varepsilon F$, where the electric displacement D is proportional to the applied field F, with the response being determined by the material dielectric constant ε. The polarization, $P = D - \varepsilon_0 F$, of the material is the increment of D above the vacuum field, and the electric susceptibility χ is defined by $P = \varepsilon_0\chi F$. For a nonlinear material $\chi = \chi^{(1)} + \chi^{(2)}F + \chi^{(3)}F^2 + \ldots$, where $\chi^{(1)}$ is the polarizability, $\chi^{(2)}$ is the hyperpolarizability, $\chi^{(3)}$ is the second-order hyperpolarizability, etc.

In general, materials are more complex than these simple scalar equations describe. The $\chi^{(\nu)}$ terms are complex valued tensors and should be treated as response kernels such that[35]

$$P_a(t) = \varepsilon_0\{\int_{-\infty}^{t}\chi_{ab}^{(1)}(t-t')F_b(t') + \int_{-\infty}^{t}\int_{-\infty}^{t}\chi_{abc}^{(2)}(t-t',t-t'')F_b(t')F_c(t'') + \cdots\} \quad (4)$$

The Fourier transform of this equation gives

$$P_a(\omega) = \varepsilon_0\left\{\chi_{ab}^{(1)}(\omega)F_b(\omega) + \frac{1}{2\pi}\int\chi_{abc}^{(2)}(\omega-\omega',\omega')F_b(\omega-\omega')F_c(\omega')d\omega' + \cdots\right\} \quad (5)$$

where the summation convention has been used for repeated tensor indices. The imaginary parts of the response functions are responsible for absorption of radiation. Frequency-dependent quantities are the most useful for experimental work and are typically calculated with standard quantum mechanical methods. These methods ordinarily evaluate the wave functions at a single frequency. "Real-time" methods are being developed to solve for the wave function in the time domain. This is a rapidly developing field and several new techniques are emerging, promising higher levels of accuracy and new insights.[35−39] The properties calculated by real-time methods give a spectrum of frequencies through Fourier transformation of the time dependence of the molecular wave functions. Both the standard and real-time methods will be discussed.

Molecular Quantum Mechanics. The theoretical evaluation of the polarization of noncrystalline condensed phases usually begins with the calculation of the properties of individual molecules. There are several different ways that this problem can be approached, but all begin with the Hamiltonian, H_0, for a molecule, which is then augmented or perturbed by an external potential. Typical external fields for laboratory work on ONLO materials are usually no larger than about 100 V/μm $\approx 2\times10^{-4}$ au, where "au" is the atomic unit of electric field. For practical applications the fields are much smaller. Furthermore, wavelengths are generally of order of magnitude 1 μm. This allows us to approximate the perturbation Hamiltonian as

$$H = H_0 + \sum_{i=1}^{N} q_i V(\mathbf{r}_i) = H_0 - \sum_{i=1}^{N} q_i\mathbf{r}_i\cdot\mathbf{F} = H_0 - \mu\cdot\mathbf{F} \quad (6)$$

where q_i is the charge on the ith particle (electrons and nuclei) located at $\mathbf{r}_i$, μ is the dipole moment, and $\mathbf{F}$ is the uniform electric field. This is the long wavelength limit (dipole approximation), i.e., the field strength is uniform over molecular dimensions. If the frequency dependence is required the field must be written as the time-dependent field $\mathbf{F} = \mathbf{F}(t) \rightarrow \mathbf{F}\exp(i\omega t)$. If several different fields act at once, then

$$\mathbf{F} = \sum_j \mathbf{F}_j\exp(i\omega_j t) \quad (7)$$

A molecular system will not react instantaneously to an oscillating field; therefore, the time evolution (eq 4) must be used in real-time, time-dependent theory. The approach to solving the wave equation

$$H\psi = i\hbar\partial\psi/\partial t \quad (8)$$

sets the various methods apart from one another. The time-independent theory is the easiest to state.

Time-Independent Perturbation Theory. Time-independent perturbation theory has contributed very important insights

into the physics of NLO behavior. The Hellmann−Feynman theorem establishes that

$$\partial E/\partial \mathbf{F} = -\boldsymbol{\mu} \tag{9}$$

where E is the energy, i.e., $E=\langle\psi|H|\psi\rangle$. The energy can be differentiated any number of times to give

$$\begin{aligned} E &= E_0+\frac{\partial E}{\partial F_a}F_a+\frac{1}{2!}\frac{\partial^2 E}{\partial F_a\partial F_b}F_aF_b+\frac{1}{3!}\frac{\partial^3 E}{\partial F_a\partial F_b\partial F_c}F_aF_bF_c \\ &+\cdots = E_0-\mu_aF_a-\frac{1}{2!}\alpha_{ab}F_aF_b-\frac{1}{3!}\beta_{abc}F_aF_bF_c \\ &-\frac{1}{4!}\gamma_{abcd}F_aF_bF_cF_d+\cdots \end{aligned} \tag{10}$$

From eq 10, it follows that

$$\begin{aligned} -\partial E/\partial F_a &= \mu_a(\mathbf{F}) \\ &= \mu_a^0+\alpha_{ab}F_b+\frac{1}{2!}\beta_{abc}F_bF_c+\frac{1}{3!}\gamma_{abcd}F_bF_cF_d+\cdots \end{aligned} \tag{11}$$

The second version of (eq 10) defines electric field coefficients, polarizability α_{ab}, hyperpolarizability β_{abc}, second hyperpolarizability γ_{abcd}, etc., in the "Taylor series convention." If the factorials in (eq 11) are absorbed into the coefficients so that β(Taylor)/2! = β(Perturbation), etc., in eq 11, the "perturbation series convention" is used. The different choices for numerical coefficients have caused considerable confusion in the literature.[40,41]

Development of the perturbation series (using Rayleigh−Schrödinger Perturbation Theory, where $\langle\psi_r|\mu_a|\psi_s\rangle = \mu_{rs,a}$) for the energy gives

$$\alpha_{ab} = 2\sum_e \frac{\mu_a\mu_b}{E_e-E_0} = 2\sum_e \frac{\mu_{0e,\,a}\mu_{e0,\,b}}{E_e-E_0} \tag{12}$$

and

$$\beta_{abc} = \underset{abc}{\mathrm{sym}}\sum_e\sum_{e'}\frac{\mu_{0e,\,a}(\mu_{ee',\,b}-\mu_{00,\,b}\delta_{ee'})\mu_{e'0,\,c}}{(E_e-E_0)(E_{e'}-E_0)} \tag{13}$$

in atomic units. The matrix elements $\langle\psi_r|\mu_a|\psi_s\rangle$ are the components of the dipole vector in state r for $r = s$, and of the transition moment vector for $r \neq s$. The sym operator is shorthand for terms arising from permutation of the tensor indices. The sums in eqs 12 and 13 are over all excited states of the unperturbed system.

Sum Over States. The perturbation theory equations provide the framework for computation of NLO properties by summation over excited states (SOS). This method has been used successfully by several groups[42−45] within the INDO (Intermediate Neglect of Differential Overlap) method for a number of years to calculate α, β, and γ. The seminal papers discussing the relationship between the polarization functions and bond length alternation (BLA) of merocyanine dyes were based on SOS methods.[42,46]

Finite Field Methods. The perturbation of the energy or charge density of a molecule that is induced by an external field is formalized in eqs 10 or 11, respectively. Both nuclei and electrons move in the presence of an external field, but it is common practice to hold nuclei fixed when calculating the changes in dipole moment that are induced by the application of a field.[47] The separation of electronic and nuclear responses to external fields is essentially an adiabatic approximation. Molecular geometry is sensitive to the solvent reaction field, for example, and many calculations have been reported in which geometries are optimized in the presence of a solvent reaction field, with subsequent determination of the electronic response using the solvent-perturbed but static geometry. It is the fast electronic response that motivates the development of ONLO materials, which justifies the use of the adiabatic approximation to capture these phenomena in calculations. Tripathy, et al. have shown that vibrations contribute only a few percent to the hyperpolarizability of DR1.[48] Many quantum codes have implementations for external fields, enabling the user to specify the orientation and strength of several different fields as required to extract numerical derivatives of the energies or dipole vectors to determine α, β, γ, etc. The user of these codes is faced with a vast array of options for calculations; choices can be made among many different methods: Hartree−Fock, density functional theory (DFT) with many different functionals, Møller−Plesset perturbation theory, coupled cluster, etc. With any choice of method, there are scores of different basis sets that might be considered. Which of these combinations is useful for a given class of problems depends upon the demands for accuracy and computational cost (usually determined by the number of electrons in the calculation). Comparisons between different methods are available.[49−51]

Analytic Derivative Methods. Although the finite field method is easy to grasp and efficient, analytical methods for computing the polarization functions have been developed. These "analytic derivative" methods, in which derivatives of the Hartree−Fock or Kohn−Sham equation are developed up to sufficiently high orders, enable the functions of interest to be evaluated directly at zero field strength.[52,53] The algebraically complex equations that result have been (gratefully) encoded by the developers so that users interested in developing ONLO molecules do not have to also develop quantum codes. Results obtained by us using both the finite field and analytic derivative methods (using the same functional) are found to be consistent with one another to within expected numerical accuracy (routinely better than ±1% agreement between methods).

To this point, we have discussed three different methods for evaluating the polarization functions: sum-over-states, finite field, and analytic derivatives. The method of choice will largely depend on the accessibility of the computer codes and the type of response function that is needed. For example, when surveying a list of structures, it may be sufficient to locate those with the most interesting properties and use only a few external field settings in a finite field method. The design of practical chromophores for EO applications requires that optical absorbances not be located too near to telecom frequencies. To assess the impact

of resonance enhancement in these cases, a frequency calculation will be useful.

Frequency-Dependent Methods. The evaluation of the frequency-dependent properties of chromophores requires the use of time-dependent theory, either perturbation theory or analytic derivatives. Suppose that the field is given by the real form[54]

$$\mathbf{F} = \mathbf{F}_0 + \mathbf{F}_\omega \cos(\omega t) \tag{14}$$

where $\mathbf{F}_0$ is a static field component and ω is the frequency of the time-dependent part. When combined with eq 11, this gives (summation convention)

$$\begin{aligned}\mu_a &= \mu_a(\omega, \mathbf{F}_0, \mathbf{F}_\omega) \\ &= \mu_a^0 + \alpha_{ab}(0;0)F_{0b} + \alpha_{ab}(-\omega;\omega)F_{\omega b}\cos(\omega t) \\ &+ \frac{1}{2}\beta_{abc}(0;0,0)F_{0b}F_{0c} + \frac{1}{4}\beta_{abc}(0;-\omega,\omega)F_{\omega b}F_{\omega c} \\ &+ \beta_{abc}(-\omega;0,\omega)F_{0b}F_{\omega c}\cos(\omega t) \\ &+ \frac{1}{4}\beta_{abc}(-2\omega;\omega,\omega)F_{\omega b}F_{\omega c}\cos(2\omega t) + \cdots\end{aligned}$$

This shows that several different functions can be extracted from a single frequency dependent calculation. To clarify, the static and frequency-dependent polarizabilities are $\alpha_{ab}(0;0)$ and $\alpha_{ab}(-\omega;\omega)$, respectively. The second-order terms are all useful and readily identified by their associated field components: $\beta_{abc}(0;-\omega,\omega)$ is pertinent for optical rectification, $\beta_{abc}(-\omega;0,\omega)$ is the quantity of interest for the Pockels effect, and $\beta_{abc}(-2\omega;\omega,\omega)$ is needed for calculation of hyper-Rayleigh scattering and second harmonic generation.

Hartree−Fock Theory. The Hartree−Fock (HF) method was important in the early development of ONLO molecules. One of the early benchmark calculations on *p*-nitroaniline was done with HF[47] (as well as MP2). Our comparative study[49] of HF, INDO, and two different density functional (DFT) methods showed generally good agreement between HF and DFT methods for dipole moments and polarizabilities, but HF typically gives smaller hyperpolarizabilities than DFT. Larger molecules become increasingly more expensive to calculate with HF, so the method is gradually being supplanted by DFT—especially popular are hybrid methods that mix some exact exchange from an HF-type calculation with the exchange correlational functional of DFT.

Density Functional Theory (DFT). The development of DFT methods has enabled relatively high accuracy calculations to be done on quite large molecules. As noted above, there will be a general increase in the magnitude of the hyperpolarizability of a homologous series of molecules as the molecules become larger. The scaling of methods with the number of electrons is about the same for HF as for DFT, so there is no reason to prefer DFT on that account. However, fairly comprehensive studies[55,56] of the energetics of reactions have shown that DFT with generalized gradient (GGA) functionals, especially with hybrid methods, perform better than HF. It is imprudent to infer that derivatives of the energy (with respect to electric field) will likewise be computed more accurately than HF on the basis of this comparison alone. Recent studies[57,58] have questioned the reliability of hyperpolarizabilities calculated with DFT. There are continuing developments in the wave functions vs electron density controversy, which we simply note here and leave for others to assess. For routine work, we prefer to use a hybrid method, as do many practical computational chemists; hybrid methods compensate for the opposing shortcomings in both HF and DFT. These methods seem to give fairly reasonable results, especially when used in the context of TD-DFT.

Time-Dependent DFT (TD-DFT). The conversion from time-independent to time-dependent HF theory is relatively straightforward (but remarkably intricate nonetheless) and involves making the MO coefficients time dependent. For DFT the situation is different, and requires modification of the fundamentals of the Kohn-Hohenberg derivation. This was done as recently as 1984 by Runge and Gross.[59] A very fruitful approach based on the Runge−Gross theorem, but using the density matrix, was taken by Furche and Ahlrichs.[60,61] These developments have led to the TD option being available in the standard DFT and hybrid codes for calculation of excited state properties, including frequency-dependent properties. Representative results obtained with the frequency dependence implemented in Gaussian09 are contained in Table 1. These results show the importance of solvent effects as well as frequency on the hyperpolarizability. It should be noted that the permutation of tensor elements that is inherent in the time-independent theory is replaced by a symmetry that couples frequencies and tensor indices in the time-dependent formulation. This is generally inconsequential for the Pockels effect, where only one tensor element is of interest, or the hyper-Rayleigh scattering experiment, where rotational averaging mixes the tensor components.

Real-Time TD-DFT. The direct integration of the time dependent Schrödinger or Kohn−Sham equation is now possible with the high-performance computing power that has become available within the past few years. This has given an unprecedented picture of a variety of processes, including electron reorganization during a chemical reaction.[62] Application of an external time-dependent field having various strengths and orientations relative to the molecular axes (time-dependent finite field method) enables evaluation of the real and imaginary parts of the response functions defined by (eq 5). The inverse relation between the time and frequency windows, inherent in the Fourier transform, requires lengthy runs for low energy processes (such as those found in chromophores intended for NLO applications) making these calculations expensive.[35] We anticipate that as these methods continue to be developed,[37,38] they will become indispensable tools for determination of the properties of ONLO systems.

Two-State Model (TSM). A two state approximation to the sum-overstates (SOS) equations, 12 and 13, is frequently used to guide insight into the critical physics that

Table 1. Frequency-Dependent Hyperpolarizability of YLD124 at 1310 and 1906 nm

solvent	ε	$\beta_{HRS}(-2\omega;\omega,\omega)$ ($\times 10^{-30}$ esu)	$\beta_{zzz}(-\omega;\omega,0)$ ($\times 10^{-30}$ esu)	$\beta_{zzz}(0;0,0)/10^{-30}$ 10^{-30} esu
		1310 nm		
vacuum	1.00	3491	702	428
carbon tet.	2.228	3601	1567	816
chloroform	4.711	2283	2388	1086
		1906 nm		
chloroform	4.711	1742	1510	1086

controls the magnitude of the first hyperpolarizability. For many ONLO molecules, the tensors are dominated by the components along the z-axis. Scalar measures of the electrical response functions, such as the trace of the polarizability tensor, might also be cast in a simplified scalar form. If only one excited state term ($e = 1$) is retained in eqs 12 and 13), we have (omitting the direction subscript and all numerical factors)

$$\alpha = \frac{\mu_{10}^2}{E_{10}} \text{ and } \beta = \frac{\mu_{10}^2 \Delta\mu_{10}}{E_{10}^2}. \quad (15)$$

Here $E_{10} = E_1 - E_0$ and $\Delta\mu_{10} = \mu_{11} - \mu_{00}$.

An additional equation that is helpful in this analysis is the oscillator strength, $f = E_{10}\mu_{10}^2$ (in atomic units) for the lowest energy transition.[63]

Experiments show that the refractive index (away from absorption) of ONLO chromophores is not unusually large. In this case, we can utilize the Clausius−Mossotti (CM) equation

$$\frac{\frac{\varepsilon}{\varepsilon_o} - 1}{\frac{\varepsilon}{\varepsilon_o} + 2} = \frac{\alpha}{v} \quad (16)$$

which relates the dielectric, ε, and the vacuum permittivity, ε_o, to the polarizability per unit volume, α/v, of a molecule. For a homologous series of molecules, the polarizability, α, increases in (approximate) proportion to the molar mass.[53] The validity of this assertion is the basis for well-known group additivity methods used to calculate polarizabilities. The apparent power law dependence seen for oligoacetylenes reflects the changing dielectric constants for these small molecules.[64] However, for long chains, the behavior has to be asymptotic, as was shown by Tretiak, et al.[65] That is, μ_{10}^2/E_{10} can be substantially increased only by increasing the size of the molecule. Conversely, for a given molar mass, large values of the hyperpolarizability can only be obtained when the $\Delta\mu_{10}/E_{10}$ term in $\beta = \alpha(\Delta\mu_{10}/E_{10})$ is large. This is achieved when the overlap of electron densities between the HOMO and LUMO is as small as possible and/or the energy gap is made small, resulting in absorption far to the red. However, significant absorption too far to the red will lead to unacceptable power losses. The molecular design goal is to find a happy medium where the lowest energy molecular absorption is as far to the red as possible while not so far as to lead to significant absorption at telecom wavelengths.

Statistical Mechanics and Acentric Order

If chromophores are treated as point dipoles and an analytical form is assumed for the potential function representing chromophore intermolecular dipole−dipole interactions, an analytical expression for the acentric order parameter is readily calculated; namely, $\langle\cos^3\theta\rangle \propto L_3(f)[1 - L_1(W/kT)^2]$ where L_n is the nth-order Langevin function; $f = (\mu g(0)F(0))/(kT)$ is the dimensionless quantity related to the energy due to the interaction of the field and the dipole; and W is the dipole−dipole interaction energy.[66] This simple form suggests that the acentric order parameter decreases nonlinearly with increasing chromophore number density (N) (because W is quadratically dependent on N). Thus, electro-optic activity will go through a maximum with number density and the position of the maximum will shift to lower N with increasing chromophore dipole moment μ (see Figure 3).

The effect of chromophore shape is treated in this simple picture by modifying the limits of integration over the orientation variable of each dipole, which takes into account the fact that chromophores cannot interpenetrate.[67] This is a regular lattice model, so when the ellipsoid is more prolate, the orientation with respect to the poling field is more restricted. This simple treatment provides reasonable simulation of the behavior of simple chromophore/polymer composite materials.[4−14,68]

A more rigorous approach to the problem is to employ fully atomistic Monte Carlo or molecular dynamics calculations.[69−72] For chromophore/polymer composites, a weak interaction between chromophores and host polymer is predicted and demonstrated in simple coarse grained rigid body calculations[67,68] and with measurements of lattice dimensionality effects.

The problem with fully atomistic methods is that they are difficult to apply to large systems. Even for simple organic electro-optic materials, they are expensive and time-consuming. Robinson and co-workers[10,25−27,30,73,74] have extended the coarse-grained treatment of chromophores described above to the development of pseudoatomistic methods. In such an approach, a fully atomistic treatment is carried out for flexible segments of the material; but rigid conjugated π-electron segments are treated as rigid geometric objects in which the nuclear coordinates are frozen at the energy minimum and the terms in the force field that correspond to internal motions are removed from the statistical mechanical energy computations (in statistical mechanics this is referred to as the united atom approximation). In addition to the molecular structure, the associated charge distributions and dipole moments are obtained

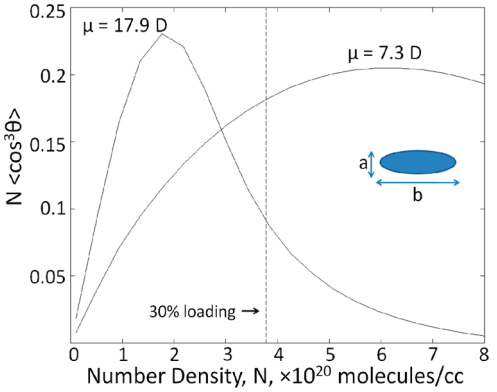

Figure 3. The theoretical relationship between $N\langle\cos^3\theta\rangle$ (loading parameter) and chromophore number density for prolate ellipsoids is shown. Both chromophore shape and dipole−dipole interactions are taken into account in the simulation. For ellipsoids of higher dipole moment, the stronger dipole−dipole interactions cap the number density that can be achieved in a macroscopic system of chromophores before electro-optic activity is seriously attenuated. For prolate ellipsoids with much smaller dipole moments, significantly higher number densities are able to be achieved and tolerated. Dimensions for the prolate ellipsoids used for these calculations were a = 8.5 Å and b = 23.3 Å. The poling field strength was taken as F = 100 V/μm.[68]

from quantum mechanical calculations. This approach has been successful not only for prediction of electro-optic activity of complex covalently incorporated chromophore materials (such as multichromophore-containing dendrimers) but also has permitted quantitative prediction of the dielectric permittivity of materials ranging from dipolar liquids (acetonitrile)[75] to multichromophore-containing dendrimers.[11,12,76] Essential to the success of pseudo-atomistic methods is the utilization of data from quantum mechanics. Combining quantum and statistical mechanical methods, a first principles simulation of electro-optic activity can be said to be achieved.

Coarse-grained statistical mechanical calculations have achieved considerable success in rationalizing the behavior of all three classes of OEO materials. For chromophore/polymer composite materials, chromophore shape is predicted and observed to be the dominant factor in determining maximum achievable electro-optic activity.[4−14,66−68,77] Chromophores exhibit only weak interaction with polymer backbone motions and behave, under poling conditions, as if they were reorienting in a three-dimensional Langevin lattice. Electro-optic activity is observed to go through a maximum with chromophore number density with the position of the maximum depending on chromophore shape and dipole moment (see Figure 3).

The behavior of polymers and dendrimers, containing covalently incorporated chromophores, depends on covalent bond potentials coupling chromophores to the surrounding macromolecular lattice. If chromophores are coupled by long flexible segments, their behavior resembles that of chromophore/polymer composite materials. However, when chromophores exist as components of multichromophore-containing dendrimers with appropriately chosen lengths of connecting flexible chain segments, a linear dependence is observed for the variation of electro-optic activity with chromophore number density (achieved by synthesizing dendrimers of different generations).[10,25,27] In these instances, chromophores behave as if they were independent particles diffusing in a 3D lattice. More specifically, the entire dendrimer undergoes 3D reorientation (in which chromophores may or may not reorient due to dendrimer linkages). Covalent bond restrictions on chromophore movement in multichromophore dendrimers can lead to reduced acentric order relative to that of isolated, independent chromophores at low concentrations reorienting in a Langevin lattice. However, because very high chromophore loading (e.g., 7×10^{20} chromphores/cc) is achieved in the dendrimer systems, an overall improvement in electro-optic activity is observed. That is, the slope of electro-optic activity versus chromophore number density plot for multichromophore dendrimers is lower than that of the same chromophore in a chromophore/polymer composite at low number density. However, the slope remains linear for the multichromophore dendrimer material while the graph goes through a maximum and electro-optic activity decreases with increasing chromophore number density for the chromophore/polymer composite material. At high chromophore loading these two plots cross and the electro-optic activity of the dendrimer material exceeds that of the chromophore/polymer composite.

Matrix-assisted-poling (MAP) materials lead to electro-optic activity that is greater than the two preceding cases for the same chromophore concentration. This result can be explained in terms of a lattice dimensionality effect that will be discussed at greater length shortly. To carry out such a discussion, insights into experimental characterization techniques are needed.

Experimental Techniques

To fully understand electro-optic activity in organic materials, reliable measurements of molecular first hyperpolarizability, $\beta(\omega,\varepsilon)$; electro-optic activity, r_{33}; poling-induced order, $\langle\cos^3\theta\rangle$ and $\langle\cos^2\theta\rangle$; dielectric permittivity, ε; and index of refraction, n, must be executed.

Molecular first hyperpolarizabilities are typically measured by hyper-Rayleigh scattering (HRS) or by electrical-field-induced second harmonic generation (EFISH).[4−14,78−80] Both of these measurements are difficult and complex. For example, HRS measurements are complicated by two-photon fluorescence, which typically requires that femtosecond, variable-wavelength HRS measurements be carried out.[78] The β value measured by HRS, $\beta_{HRS}(-2\omega;\omega,\omega)$ is an averaged value and requires theory to be used to relate this to β_{zzz}, the value relevant for electro-optic device applications. EFISH measurements yield the product of dipole moment (μ) and molecular first hyperpolarizability (β_{zzz}) and are complicated by a contribution from molecular second hyperpolarizability (γ). Both measurements are time-consuming and require study of electro-optic chromophores for a number of chromophore concentrations in solvents such as chloroform. In general, the spectral dispersion of molecular first hyperpolarizability must be investigated and the dependence of host dielectric permittivity must be defined.

Reasonable agreement between theory and experiment is obtained for many commonly utilized OEO chromophores although some controversy still exists for more exotic chromophores.[10] Recently, more detailed studies of the effects of optical frequency and dielectric permittivity dependences of molecular first hyperpolarizability have been carried out.[10,12,76] Such studies are important for the quantitative understanding of factors that contribute to macroscopic electro-optic activity.

Ellipsometry in the form of the Teng-Man technique[10,81,82] has been the most commonly used method of measuring the electro-optic coefficient r_{33}. However, it has been shown that for thin films of OEO materials on indium tin oxide (ITO) substrates (a multi-interface structure), substantial errors can arise.[83] Moreover, the Teng-Man technique requires assumptions about the relative magnitudes of r_{33} and r_{13} in order to extract a value for r_{33}. The major attraction of the Teng-Man method is its ease of implementation. A more reliable technique is the attenuated total reflection (ATR) method, which permits measurement of both r_{33} and r_{13}.[10,82] The ATR technique is more invasive, carrying the potential for sample damage and requires use of a high index of refraction (rutile) prism for chromophores characterized by high index of refraction.[10] However, because of the improved accuracy afforded by the ATR technique, the discussions of electro-optic activity presented here are restricted to consideration of ATR data.

Electro-optic activity can be related to acentric order through (eq 1). This requires knowledge of β, dielectric permittivity (ε), and index of refraction (n). From these experimentally obtained parameters, $\langle\cos^3\theta\rangle$ can be calculated, but it is an indirect measurement. The ratio r_{33}/r_{13} provides a more direct measurement of acentric order parameter as long as the anisotropy of β is estimated from theory or experimentally measured.

Another route to understanding poling-induced order beyond estimation of $\langle\cos^3\theta\rangle$ is to measure $\langle P_2\rangle$ or $\langle\cos^2\theta\rangle$, the centrosymmetric order parameter. Because the order induced by action of the poling field is reflected in all order parameters (both even and odd powers of $\cos\theta$), centrosymmetric order parameters are also useful for understanding poling-induced order. $\langle P_2\rangle$ has traditionally been measured experimentally by the normal incidence method (NIM) or by variable angle polarized absorption spectroscopy (VAPAS).[84] Recently, we have modified the VAPAS technique by referencing the absorption of p-polarized light to the absorption of s-polarized light.[85] The absorption of p-polarized light depends on poling-induced order (tilt angle), whereas the absorption of s-polarized light does not depend on tilt angle and acts as a reference. The use of this ratio method corrects for many measurement artifacts, such as Fresnel reflections, associated with a multilayer sample (glass/ITO/EO material). We refer to this new technique as variable angle polarization referenced absorption spectroscopy (VAPRAS). We also take into account that OEO materials are strongly absorbing in the analysis of VAPRAS data: full Jones matrix analysis is carried out.[86] VAPRAS measurements are complemented by variable-angle spectroscopic ellipsometry (VASE) measurements.[87,88]

Standard absorption measurements are unable to detect the coumarin units in a thin film device structure (higher dielectric environment) because of absorption of the glass and ITO in the UV spectral range. For comparison, UV−visible absorption spectroscopy data are shown with typical VASE data (for the C1 dendrimer material) in Figure 4.

As is shown in Figure 4, VASE permits measurement of the relative orientations of components of the chromophore and coumarin-containing dendrimer. For the example of C1, the chromophore and coumarin units are approximately orthogonal. VASE also provides index of refraction data in all layers useful for the analysis of VAPRAS experiments.

If phases of reduced dimensionality exist below the material glass-transition temperature, it is possible that these may be detected by nanoscopic viscoelastic measurements such as shear modulation force microscopy (SM-FM), intrinsic friction analysis (IFA), and dielectric relaxation spectroscopy (DRS). The details of these experimental measurements are given elsewhere[89−92] but as noted in the next section, these provide complementary evidence for the existence of dendrimer cooperativity, leading to reduction in effective lattice dimensionality in the macroscopic system of electro-optic chromophores. This is found to be the case for the HDFD and C1 chromophores of Figure 2.[89−93]

Effect of Lattice Dimensionality

The order parameters $\langle P_2\rangle$ and $\langle\cos^3\theta\rangle$ are related through the effective dimensionality of the material lattice surrounding the OEO chromophore.[30] For 2D and 3D lattices, the expressions for $\langle\cos^2\theta\rangle$ and $\langle\cos^3\theta\rangle$ are given in terms of Bessel functions in Table 2.[10]

For the three-dimensional case, one can show (numerically) for the independent dipole model that $\langle\cos^3\theta\rangle_{3D} \approx \sqrt{\frac{3}{5}\langle P_2\rangle_{3D}}$ for any value of the poling strength. A similar relation exists for the 2D case, and may exist for a system of noninteger dimensionality, M, $2 \le M \le 3$. The order parameter relation may be generalized by

$$\langle\cos^3\theta\rangle_{MD} \approx \sqrt{\left(\frac{9-2M}{2+M}\right)\left(\langle P_2\rangle_{MD} - \frac{3-M}{2M}\right)} \quad (17)$$

As noted in the discussion of experimental measurements, the centrosymmetric order parameter, $\langle P_2\rangle$, is directly measured by either VASE, VAPRAS, or NIM, and is distinct from the acentric order parameter.[30] $\langle P_2\rangle$ can be determined directly by VAPRAS and VASE measurements and $\langle\cos^3\theta\rangle$ can be determined indirectly by measurement of β_{zzz}, r_{33}, r_{13}, n, and ε. The experimental measurements can be compared against theoretical calculations. The values for these order parameters can then be used to estimate M. Table 3 provides a summary of parameters obtained for four systems: Two concentrations of the chromophore/polymer composite F2/PMMA, the multichromophore containing dendrimer P3, and the

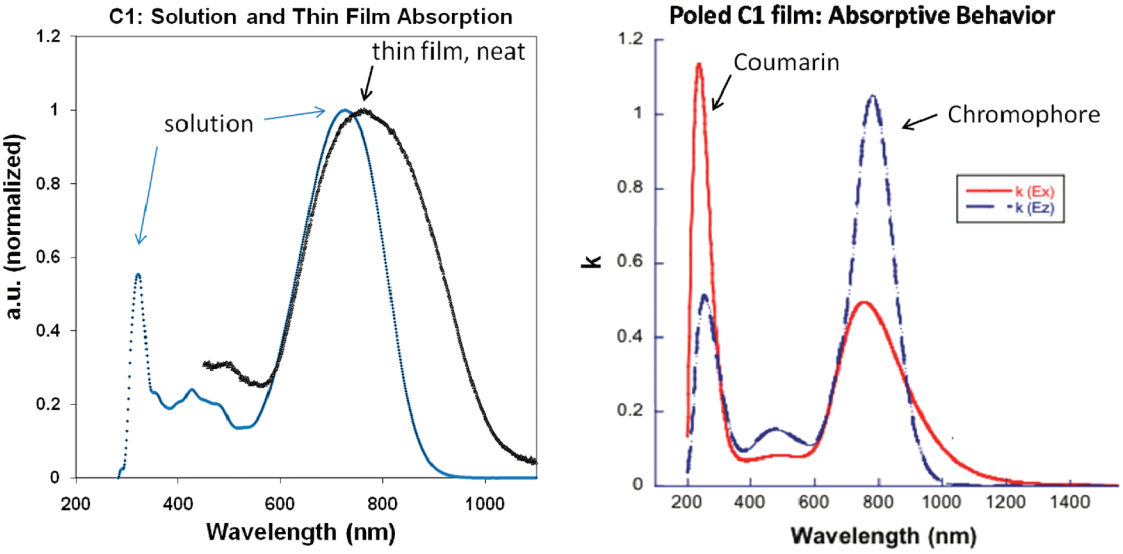

Figure 4. Left panel shows the absorption for the C1 dendrimer in chloroform solution and in a thin film, illustrating approximately where the chromophore and coumarin units distinctively absorb. Note that thin film absorption exhibits a bathochromic shift. The right panel is typical VASE data corresponding to a poled (anisotropic) sample of the C1 dendrimer. These data show the spectral anisotropy associated with both coumarin and chromophore moieties.

Table 2. Equations for Calculating Second- and Third-Degree Order Parameters for Two- And Three-Dimensional Systems Expressed in Terms of Bessel Functions $J_n(z)$[30] (poling parameter is $f = (\mu g(0)F(0))/(kT)$)

$\langle\cos^n\theta\rangle$	2D order parameters	3D order parameters
$n = 2$	$\langle\cos^2\theta\rangle_{2D} = \frac{1}{2}\left\{1 - \frac{J_2(-if)}{J_0(-if)}\right\}$	$\langle\cos^2\theta\rangle_{3D} = 1 - 2\frac{\langle\cos^1\theta\rangle_{3D}}{f}$
$n = 3$	$\langle\cos^3\theta\rangle_{2D} = \frac{3}{4}\langle\cos^1\theta\rangle_{2D} + \frac{1}{4}\frac{-iJ_3(-if)}{J_0(-if)}$	$\langle\cos^3\theta\rangle_{3D} = \frac{2}{f}\left(3\frac{\langle\cos^1\theta\rangle_{3D}}{f} - 1\right) + \langle\cos^1\theta\rangle_{3D}$

Table 3. Experimental Data Used to Estimate the Dimensionality (M) of C1, F2 in PMMA, and P3

material	r_{33}/F[a]	N[b]	r_{33}/NF[c]	$\langle P_2\rangle$[d]	$\beta_{zzz}(-\omega;0,\omega)$[e]	$g(\omega)/n^4$	$\langle\cos^3\theta\rangle$[f]	$N\langle\cos^3\theta\rangle$	M
C1 (TiO_2)	1.92 ± 0.04	4.4	0.28	0.19 ± 0.015	3000 ± 300	0.57	0.15 ± 0.02	0.66 ± 0.07	2.2
F2/PMMA	0.45 ± 0.02	1.7	0.26	0.035 ± 0.01	3500 ± 600	0.62	0.073 ± 0.01	0.12 ± 0.02	2.8
F2/PMMA[g]	0.15 ± 0.02	3.6	0.042	0.04 ± 0.02	3500 ± 600	0.57	0.015 ± 0.003	0.054 ± 0.01	2.8
P3[h]	1.42 ± 0.04	6.4	0.22	0.019 ± 0.005	4033[i] ± 126	0.52	0.063 ± 0.003	0.41 ± 0.02	2.9

[a] $(nm/V)^2$. [b] $N \times 10^{20}$molecules/cc. [c] $(nm/V)^2(cc/10^{20}$ molecules). [d] $\langle P_2\rangle$ at $F = 50$ V/μm for C1, low-density F2/PMMA, and P3; $E_p = 60$ V/μm for high-density F2/PMMA. [e] $\beta_{zzz}(-\omega;0,\omega) \times 10^{30}$ esu. [f] All $\langle\cos^3\theta\rangle$ values estimated from eq 1 using r_{33}/F ($F = 50$ V/μm), except for F2 at high density, where $F = 60$ V/μm. [g] $F = 60$ V/μm for F2 at high density. [h] P3 (i.e., PSLD-33) data were previously reported. [i] Theoretical value calculated using TD-DFT. F2/PMMA percentages should be noted for the two systems.

coumarin-containing dendrimer C1 (see Figure 2 for the structures of these materials). Note that the intrinsic chromophore is the same for each of these systems. A wealth of experimental data and theoretical simulations suggest that the values reported in Table 3 are reasonable numbers and support the fundamental contention that the lattice dimensionality is lower for C1 materials than for F2 and P3 materials.

The concept of reduced lattice dimensionality for C1 (and for HDFD) is also supported by thermomechanical transition and mobility analyses. Shear modulation force microscopy (SM-FM)[91] showed structural transitions (i.e., T_g) for both C1 and HDFD (see Figure 5). These transitions originated from coumarin-coumarin and arene-perfluoroarene dendrimer coupling, respectively. The dendrimer transitions were dubbed T_g (glass transition), as they correspond to calorimetric transitions observed by differential scanning calorimetry.[89] Mobility sensitive intrinsic friction analysis (IFA)[92] conducted above T_g for HDFD (Figure 6) further supports the notion of a glass forming process, by revealing high entropic co-operativities of ~73% of the total apparent energy E_a of ~70 kcal/mol. The occurrence of such high entropic contributions in the vicinity of T_g, is unique to glass forming polymers and liquid crystals.

Both C1 and HDFD also revealed low temperature transitions, T_c, which were absent for C1 modified systems that contained no dipole (i.e., NDC2 in Figure 5),[93] and are absent for a simple chromophore in a polymer host (such as YLD124 in APC, data not shown). All systems show a T_g transition, but the T_c transition is only seen in systems with pendant groups attached to the chromophore. Electric field poling of C1 and HDFD revealed onsets of effective poling above T_c with maximum electro-optical activities when poled below, but near T_g. Although the reduced dimensionality structure

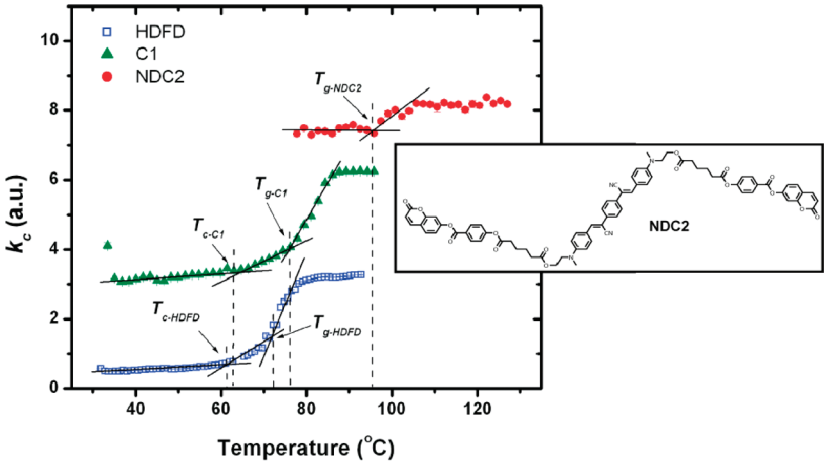

Figure 5. SM-FM analysis involving the thermomechanical contact resistance k_c: HDFD and C1 dendrimer systems are contrasted to a coumarin analogue (NDC2) that contains no dipole moiety. The molecular structure of NDC2 is shown to the right. The self-assembly transition into a glass phase is apparent for all three systems by the existence of T_g. Constrained by the matrix, the dipole containing chromophores of HDFD and C1 form a solid subphase around T_c (into a reduced lattice dimensional matrix).

is due to dendrimer interactions, the low-temperature transition T_c can be attributed to chromophore interactions. Thereby, the T_c value was found to depend on the reduced lattice dimensional matrix, as found for a set of dendritic arene stabilization moieties with identical chromophores. T_c values as high as 118 °C for anthryl-pentafluorophenyl interactions could be measured.[90] Although coincidental, it is interesting to note that C1 and HDFD behave comparably in terms of the thermal transition property T_c, which suggests a similarly dense structure of the two systems.

IFA reveals for the intermediate phase regime ($T_c < T < T_g$) a highly cooperative submolecular rotational mobility of the chromophores, as illustrated for HDFD in Figure 6, which identifies T_c as the chromophore stabilization temperature. Below T_c, the rotational modes are frozen. Only the thermally active and noncooperative enthalpic modes of the reduced lattice dimensional matrix are observed from the IFA energy signature (e.g., 23 kcal/mol for HDFD in Figure 6).

It is interesting to note that the high apparent activation energy in the intermediate phase regime (44 kcal/mol for HDFD) carries a substantial amount of entropic contribution (~50%), indicating that the chromophores are not only densely packed and motion constrained, but also reduced in their freedom of rotational motion.

Taken together, order parameter measurements and SM-FM/IFA data provide insights into the structural and energetic aspects of specific spatially anisotropic intermolecular electrostatic interactions that impact lattice dimensionality and, in turn, impact poling efficiency and macroscopic electro-optic activity.

C1 and HDFD materials represent only two examples of MAP materials. Other materials, which have yet to be extensively studied, include binary chromophore organic glasses (BCOGs) and the optically assisted electric field poling of chromophores doped into DR1-co-PMMA (Figure 2).[10,29,32,33]

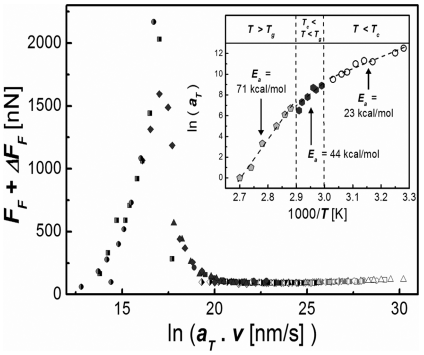

Figure 6. IFA master curve for HDFD. Inset: Arrhenius analysis of the thermal shift factor a_T reveals the energetics of thermally active molecular and submolecular entities. Adopted and modified with permission from ref 89. Copyright 2008 American Chemical Society.

Other Considerations

Conductivity. As the number density of chromophores is increased in a material, conductivity under electric field poling conditions becomes a problem and poling field strengths can be limited to less than 70 V/micrometer to avoid runaway conductivity and sample damage. A number of researchers have noted this phenomenon and have shown that conductivity effects can be reduced by depositing nanoscopic (50−200 nm) layers of TiO_2 between the organic electro-optic material and the ITO electrode.[12,94] Conductivity problems are particularly severe for OEO materials integrated into nanoslot doped silicon photonic waveguide devices and for materials undergoing optically assisted poling. Conductivity issues, together with problems of chromophore decomposition under poling conditions, have necessitated use of careful procedures to achieve effective electric field poling. Subtle variations in poling temperature and electric field strengths can lead to disastrous results. Issues associated with poling have greatly inhibited achievement of the full potential of the very large molecular first hyperpolarizabilities that exist for currently available OEO chromophores.

Thermal and Photostability. One of the most direct ways to improve both thermal and photochemical stability of organic electro-optic materials is to introduce covalent cross-links between chromophore-containing moieties. In early studies of OEO materials, such cross-linking was normally accomplished by utilizing condensation reactions.[95] More recently, cycloaddition reactions have largely replaced these earlier methods. The two commonly utilized cycloaddition reactions include (1) reaction of fluorovinyl ether groups to form cyclobutyl cross-links[28,96−99] and (2) Diels−Alder/retro-Diels−Alder reaction of dienes and dienophiles.[10,100−104] The latter has become very popular because of the wide range of diene and dienophiles available, which can be used to widely tune the glass-transition temperatures of materials. Utilizing this methodology, electro-optic materials have been produced with glass-transition temperatures exceeding 200 °C.[102,103]

Lumera Corporation has produced devices fabricated from OEO materials that have passed Telcordia standards,[105−107] significantly addressing one of the lingering concerns related to OEO materials.

Device Considerations.

Fabrication. A unique advantage of OEO materials is the variety of processing options that can be pursued and the compatibility of materials with a diverse range of substrate materials. OEO materials can be deposited both from solution (e.g., spin-casting, crystal growth, sequential synthesis methods) and the vapor phase. OEO materials are amendable to processing by nanoimprint and soft lithography techniques[108] and thus are amenable to the low-cost, mass production of devices. Conformal and flexible devices can be fabricated by lift-off techniques.[109]

Performance. The bandwidth performance of devices fabricated from OEO materials is typically not determined by the fundamental response of the OEO material to applied time-dependent electrical fields, but is rather determined by the resistivity of the electrodes used to supply the radiofrequency/microwave/millimeterwave fields to the sample. With the exceptions of optical rectification, frequency doubling, and difference frequency (e.g., THz generation and detection) applications, the full bandwidth potential of organic second order nonlinear optical materials is likely to be unrealized in devices. However, high bandwidth (including 100 Gigabits per second) devices have already been demonstrated; thus, devices in this range will likely become more common.[107,110,111] Moreover, the fast response time of OEO materials can be traded for improved sensitivity (i.e., reduced drive voltages) in resonant devices such as ring microresonators and etalons. Many such devices have already been demonstrated.[15−20,112−116]

Advances in device engineering have played a major role in enhancing the performance of materials such as lithium niobate and the same should likely be true for OEO materials. Already, OEO materials have been successfully integrated with nanoslot silicon photonic waveguide structures. More sophisticated structures are certain to be produced in the future.[15−20] In particular, the large electro-optic activity that can potentially be achieved with OEO materials should permit dramatic reduction in the size of EO devices, making them more compatible and integrable with the dimensions of chipscale silicon electronics.

Conclusions and Future Prospects

In the 1990s, the molecular hyperpolarizability of EO chromophores increased at a rapid rate with the introduction of new and improved chromophores culminating with the synthesis of chromophores containing tricyanovinylfuran (TCF)-type acceptors and isophorone-protected polyene bridges (YLD-124 type chromophores—see Figure 2).[117,118] Surprisingly, these chromophores still represent the state-of-the-art for the fabrication of devices with their hyperpolarizability and stability continuing to be improved somewhat by fine-tuning of substituents, e.g., at the 2-position of the isophorone ring and at various points in the acceptor.[119] However, there is no reason to believe that such chromophores represent the ultimate in molecular hyperpolarizability that can be achieved. The hyperpolarizability of even the best chromophore to date is still more than an order of magnitude below the limit suggested by Kuzyk.[48,120,121] Twisted bridge chromophores developed by Tobin Marks and co-workers[122−125] have been predicted (and experimentally observed by EFISH) to exhibit large molecular first hyperpolarizabilities. These chromophores, where the molecular hyperpolarizability is defined by an admixture of "neutral ground state", "zwitterionic ground state", and "singlet biradical ground state" contributions,[126] have yet to be translated to prototype device fabrication. Part of the problem inhibiting this transition is the strong tendency for these chromophores to aggregate. Octupolar EO chromophores can potentially solve problems associated with dipolar chromophores and continue to be investigated[127−131] but have yet to be used for device applications.

Recently, researchers have turned attention to investigating the effect of dielectric permittivity on the observed molecular first hyperpolarizability of chromophores.[10,75,76] Dielectric permittivity effects have been shown to be potentially large and used to enhance the macroscopic electro-optic activity of materials.

Improvement of molecular hyperpolarizability has typically been accompanied by increased chromophore dipole moment and a corresponding decrease in acentric order parameters for chromophore/polymer composite materials (see Figure 3). Because of the attenuation of acentric order with increasing chromophore number density, chromophore loadings typically have had to be kept below 25% (weight guest chromophore/weight polymer host). The combination of low chromophore number densities and low acentric order parameters (<0.15) restricted electro-optic coefficients to modest values (<30 pm/V). The realization that chromophore shape could play a role in improving poling efficiency led to an improvement in acentric order and electro-optic coefficients (e.g., to values on the order of 60 pm/V).[24] The realization that covalent bond potentials could be exploited to improve chromophore number densities without the attenuation of

acentric order led to the improvement in electro-optic coefficients to 100 pm/V or greater in the last ten years.[25,27] However, for such multichromophore-containing dendrimers, the acentric order parameters were still low (see Table 3) and at low chromophore loadings were less than that achieved for chromophore/polymer composites.

MAP materials have resulted in further improvement in electro-optic activity (to values greater than 300 pm/V), attributed to the combination of increased acentric order parameters and high chromophore number densities.[29,32,33] As discussed here, this improvement can likely be attributed to a lattice dimensionality effect. The concept of MAP materials is just beginning to be exploited and it is highly likely that further improvements in EO activity will be achieved, although it may be very difficult to produce lattices of dimensionality less than 2. In particular, the combined effects of chromophore shape control, spatial restrictions associated with covalent bond potentials, and spatially anisotropic intermolecular interactions that lead to reduction of the effective lattice dimensionality have yet to be systematically exploited. It is not unreasonable that acentric order could be increased by a factor of 2 or 3 leading to electro-optic coefficients approaching 1000 pm/V. The higher number densities of multichromophore-containing dendrimers and MAP materials have led to larger index of refraction, dielectric permittivity, electronic (interband) absorption, and increased conductivity under poling conditions. These features can prove problematic for certain device designs but in general MAP materials exhibit favorable electro-optic and optical loss characteristics. For example, binary chromophore organic glasses typically exhibit reduced optical loss due to better material homogeneity associated with mixing of "polar" guest and host materials. Solvatochromic shifts are not observed as a function of varying the relative concentrations of guest and host chromophores.[32,101] Design of spatially anisotropic intermolecular interactions that improve poling efficiency must be carried out with care. Interactions cannot be so strong that movement of chromophores under the action of an electric poling field is inhibited. However, all of the materials discussed in this review yield optical loss values in the range of 1−2 dB/cm.

Material conductivity under poling conditions has been the most significant problem encountered with MAP materials. If not for the reduction in poling field strength that can be used to induce electro-optic activity, electro-optic coefficients of 600 pm/V would have already been achieved. The attenuation of electro-optic activity from conductivity has been somewhat ameliorated by the introduction of thin (charge blocking) TiO_2 layers between the OEO material and ITO electrode.[132] Of course, conductivity problems associated with electric field poling (together with the introduction of new device architectures) have given new impetus to the exploration of the fabrication of thin films of OEO materials by sequential synthesis/self-assembly and crystal growth techniques.[133−144]

Diels−Alder/retro-Diels−Alder cross-linking has provided a very useful route to electrically poled materials with glass transition temperatures on the order of 200 °C.[102,103] The choice of diene and dienophile permits wide tuning of thermal stability and thermal processing temperatures. This chemistry now appears to be a widely used method for controlling thermal and photochemical properties. The spatially anisotropic intermolecular electrostatic interactions of MAP materials also contribute to improved thermal and photochemical stability, which no longer appear to be major roadblocks to the utilization of OEO materials.[105−107]

Device engineering considerations will likely play an increasingly important role in defining the utilization of OEO materials. In particular, the advent of silicon photonics and plasmonics affords new opportunities for the utilization of OEO materials. The size (short optical/radiofrequency field interaction lengths) of devices associated with silicon photonics and plasmonics impacts the definition of acceptable optical loss and macroscopic electro-optic activity. Device concepts such as slotted waveguide structures that concentrate both optical and radiofrequency fields into sub-100 nm slots containing OEO materials could lead to a revolution in device performance. Device requirements will likely motivate utilization of a greater range of material processing options. The smaller dimensions of silicon photonic waveguide structures may encourage greater use of crystal growth and sequential synthesis/self-assembly techniques.

Slotted silicon photonic/OEO devices have already exhibited drive voltages on the order of 0.25 V. Very likely, drive voltages of less than 0.1 V will be achieved through improved device design and a better understanding of material interface issues. A number of factors determine the drive voltage to be desired. For example, Mach−Zehnder interferometric devices with a drive voltage of 0.1 V represent the transition from "loss" to "gain" in the electrical-to-optical-to-electrical signal transduction process. However, Cox and co-workers point out that the analysis of noise sources is critical to understanding the gains in performance that can be achieved by continued reduction of drive voltages.[145] In short, there will be limits on the gain that can be achieved. However, another motivation for improving electro-optic activity of OEO materials is to reduce device lengths (optical/electrical field interaction lengths). For chipscale integration of electronics and photonics, reduction in EO device dimensions is critical to achieve size compatibility between electronic and photonic components. Spatial light modulation devices also require reduced device dimensions. In short, the material electro-optic activity, optical loss, and stability properties leading to optimum device performance will vary from application (device type) to application. However, many device engineers view that an electro-optic activity of 1000 pm/V is required for a dramatic impact on the utilization of OEO materials. This would position the activity of "electronic" OEO materials between liquid crystalline materials (thousands of pm/V) and lithium niobate ($r_{33} \sim 30$ pm/V) but with orders of magnitude faster response time than these materials and with dramatically improved processing (device fabrication) options.

Very recent work on combining slotted silicon waveguide concepts and photonic crystal engineering concepts that exploit control of photon group velocities (slow wave structures) have led to very small V_π-length products.[146] Utilization of slow wave structures requires attention to optical coupling to avoid unacceptable optical loss; however, Chen and co-workers have addressed this concern with very innovative photonic crystal engineering.[146]

From a commercial standpoint, it is unlikely that OEO materials will displace lithium niobate for the manufacture of single modulator devices, particularly for applications requiring bandwidths of less than 20 GHz. Chipscale integration of photonics and electronics will likely be a significant driver for the utilization of OEO materials as will specialized applications (e.g., RF photonics, phased-array radar), which require special structures such as conformal device structures. Of course, the development and adoption of OEO materials may be dramatically influenced by global economics.

Acknowledgment. The authors acknowledge partial financial support for this research from the National Science Foundation (DMR-0905686) and the Air Force Office of Scientific Research (FA9550-09-1-0589). The authors also thank Drs. Michael Hochberg, Philip Reid, Denise Bale, Philip Sullivan, and Antao Chen; their colleagues; and many members of the Jen research group for contributing to this research and for many helpful discussions. We thank Jianing Sun at the J. A. Woollam Company for VASE measurements and Dr. Robert Nielsen for the preparation of Figure 3.

References

(1) Drenser, K. A.; Larsen, R. J.; Strohkendl, F. P.; Dalton, L. R. *J. Phys. Chem.* **1999**, *103*(14), 2290–2301.
(2) Hochberg, M.; Baehr-Jones, T.; Wang, G.; Shearn, M.; Harvard, K.; Liu, J.; Chen, B.; Shi, Z.; Lawson, R.; Sullivan, P. A.; Jen, A. K.-Y.; Dalton, L. R.; Scherer, A. *Nat. Mater.* **2006**, *5*, 703–709.
(3) McLaughlin, C. V.; Hayden, L. M.; Polishak, B.; Huang, S. M.; Luo, J. M.; Kim, T. M.; Jen., A. K. *Appl. Phys. Lett.* **2008**, *92*(15), 151107−1–3.
(4) Dalton, L. R.; Harper, A. W.; Ren, A. S.; Wang, F.; Todorova, G.; Chen, J.; Zhang, C.; Lee, M. *Ind. Eng. Chem. Res.* **1999**, *38*, 8–33.
(5) Dalton, L. R. Nonlinear optical polymeric materials: from chromophore design to commercial applications. In *Polymers for Photonics Applications I*; Springer: Berlin, 2002; Vol. *158*, pp 1−86.
(6) Dalton, L. R. *J. Phys.: Condens. Matter* **2003**, *15*, R897–R934.
(7) Dalton, L. R. Organic electro-optic materials. In *Handbook of Conducting Polymers*; Skotheim, T., Reynolds, J., Eds.; CRC Press: Boca Raton, FL, 2006; Chapter 6, pp 229−267.
(8) Cho, M. J.; Choi, D. H.; Sullivan, P. A.; Akelaitis, A. J. P.; Dalton, L. R. *Prog. Polym. Sci.* **2008**, *33*, 1013–1058.
(9) Dalton, L. R.; Sullivan, P.; Bale, D. H.; Hammond, S.; Olbricht, B. C.; Rommel, H.; Eichinger, B. E.; Robinson, B. H. Organic photonic materials. In *Tutorials in Complex Photonic Media*; Noginov, N., McCall, M. W., Dewar, G., Zheludev, N. I., Eds.; SPIE Press: Bellingham, WA, 2009; Chapter 16, pp 535−574.
(10) Dalton, L. R.; Sullivan, P. A.; Bale, D. H. *Chem. Rev.* **2010**, *110*, 25–55.
(11) Sullivan, P. A.; Dalton, L. R. *Acc. Chem. Res.* **2010**, *43*(1), 10–18.
(12) Dalton, L. R.; Sullivan, P. A.; Bale, D.; Olbricht, B.; Davies, J.; Benight, S.; Kosilkin, I.; Robinson, B. H.; Eichinger, B. E.; Jen, A. K.-Y. Organic electro-optic materials: understanding structure/function relationships critical to the optimization of electro-optic activity. In *Organic Thin Films for Photonics Applications*; Herman, W., Foulger, S., Eds.; ACS Symposium Series; American Chemical Society: Washington, D.C., 2010; Chapter 2, pp 13−33.
(13) Zhou, X. H.; Luo, J.; Kim, T. D.; Jang, S. H.; Overney, R. M.; Dalton, L. R.; Jen, A. K.-Y. Molecular design and supramolecular organization of highly efficient nonlinear optical chromophores for exceptional electro-optic properties. In *Organic Thin Films for Photonics Applications*; Herman, W., Foulger, S., Eds.; ACS Symposium Series; American Chemical Society: Washington, D.C., 2010; Chapter 4, pp 51−66.
(14) Steier, W. H.; Dalton, L. R. Polymer modulators. In *Broadband Optical Modulators: Science, Technology, and Applications*; Chen, A., Murphy, E., Eds.; Taylor & Francis: New York, submitted.
(15) Baehr-Jones, T.; Hochberg, M.; Wang, G.; Lawson, R.; Liao, Y.; Sullivan, P. A.; Dalton, L. R.; Jen, A. K.-Y.; Scherer, A. *Opt. Express* **2005**, *13*, 5216–5226.
(16) Hochberg, M.; Baehr-Jones, T.; Wang, G.; Huang, J.; Sullivan, P. A.; Dalton, L. R.; Scherer, A. *Opt. Express* **2007**, *15*, 8401–8410.
(17) Baehr-Jones, T.; Penkov, B.; Huang, J.; Sullivan, P. A.; Davies, J.; Takayesu, J.; Luo, J.; Kim, T.-D.; Dalton, L. R.; Jen, A. K.-Y.; Hochberg, M.; Scherer, A. *Appl. Phys. Lett.* **2008**, *92*, 163303−1–3.
(18) Takayesu, J.; Hochberg, M.; Baehr-Jones, T.; Chan, E.; Wang, G.; Sullivan, P. A.; Liao, Y.; Davies, J.; Dalton, L. R.; Scherer, A.; Krug, W. *IEEE J. Lightwave Technol.* **2008**, *27*(4), 440–448.
(19) Wubern, J. H.; Hampe, J.; Petrov, A.; Eich, M.; Luo, J.; Jen, A. K.-Y.; Di Falco, A.; Krauss, T. F.; Bruns, J. *Appl. Phys. Lett.* **2009**, *94*, 241107−1–3.
(20) Ding, R.; Baehr-Jones, T.; Liu, Y.; Bojko, R.; Witzens, J.; Huang, Su; Luo, J.; Benight, S.; Sullivan, P.; Fedeli, J.-M.; Fournier, M.; Dalton, L. R.; Jen, A. K.-Y.; Hochberg, M. *Opt. Express* **2010**, *18*(15), 15618–15623.
(21) Enami, Y.; Mathine, D.; DeRose, C.; Norwood, R.; Luo, J.; Jen, A. K.-Y.; Peyghambarian, N. *Appl. Phys. Lett.* **2007**, *91*, 093505−1–3.
(22) Shi, S.; Prather, D. W. *Appl. Phys. Lett.* **2010**, *96*, 201107−1–3.
(23) Dionne, J. A.; Kiest, K.; Sweatlock, L. A.; Atwater, H. A. *Nano Lett.* **2009**, *9*(2), 897–902.
(24) Shi, Y.; Zhang, C.; Zhang, H.; Bechtel, J. H.; Dalton, L. R.; Robinson, B. H.; Steier, W. H. *Science* **2000**, *288*, 119–122.
(25) Sullivan, P. A.; Rommel, H. L.; Takimoto, Y.; Hammond, S. R.; Bale, D. H.; Olbricht, B. C.; Liao, Y.; Rehr, J.; Eichinger, B. E.; Jen, A. K.-Y.; Reid, P. J.; Dalton, L. R.; Robinson, B. H. *J. Phys. Chem. B* **2009**, *113*(47), 15581–15588.
(26) Benight, S. J.; Bale, D. H.; Olbricht, B. C.; Dalton, L. R. *J. Mater. Chem.* **2009**, *19*, 7466–7475.
(27) Sullivan, P. A.; Rommel, H.; Liao, Y.; Olbricht, B. C.; Akelaitis, A. J. P.; Firestone, K. A.; Kang, J.-W.; Luo, J.; Choi, D. H.; Eichinger, B. E.; Reid, P. J.; Chen, A.; Jen, A. K.-Y.; Robinson, B. H.; Dalton, L. R. *J. Am. Chem. Soc.* **2007**, *129*, 7523–7530.
(28) Luo, J.; Haller, M.; Ma, H.; Liu, S.; Kim, T.-D.; Tian, Y.; Chen, B.; Jang, S.-H.; Dalton, L. R.; Jen, A. K.-Y. *J. Phys. Chem. B* **2004**, *108*(25), 8523–8530.
(29) Kim, T.-D.; Lao, J.; Cheng, Y.-J.; Shi, Z.; Hau, S.; Jang, S.-H.; Zhou, X.-H.; Tian, Y.; Polishak, B.; Huang, S.; Ma, H.; Dalton, L. R.; Jen, A. K.-Y. *J. Phys. Chem. C* **2008**, *112*(21), 8091–8098.
(30) Benight, S. J.; Johnson, L. E.; Barnes, R.; Olbricht, B. C.; Bale, D. H.; Reid, P. J.; Eichinger, B. E.; Dalton, L. R.; Sullivan, P. A.; Robinson, B. H. *J. Phys. Chem. B* **2010**, *114*(37), 11949–11956.
(31) Zhou, X.-H.; Luo, J.; Huang, S.; Kim, T.-D.; Shi, Z.; Cheng, Y.-J.; Jang, S.-H.; Knorr, D. B., Jr.; Overney, R. M.; Jen, A. K.-Y. *Adv. Mater.* **2009**, *21*(19), 1976–1981.
(32) Olbricht, B. C.; Sullivan, P. A.; Wen, G.-A.; Mistry, A.; Davies, J. A.; Ewy, T. R.; Eichinger, B. E.; Robinson, B. H.; Reid, P. J.; Dalton, L. R. *J. Phys. Chem. C* **2008**, *112*(21), 7983–7988.
(33) Pereverzev, Y. V.; Gunnerson, K. N.; Prezhdo, O. V.; Sullivan, P. A.; Liao, Y.; Olbricht, B. C.; Akelaitis, A. J. P.; Jen, A. K.-Y.; Dalton, L. R. *J. Phys. Chem. C* **2008**, *112*, 4355–4363.
(34) Jackson, J. D. *Classical Electrodynamics*; John Wiley: Hoboken, NJ, 1999.
(35) Takimoto, Y.; Vila, F. D.; Rehr, J. J. *J. Chem. Phys.* **2007**, 127.
(36) Takimoto, Y. A real-time time-dependent density fuctional theory method for calculating linear and nonlinear dynamic optical response. Ph.D. Dissertation, University of Washington, Seattle, WA, 2008.
(37) Christiansen, O.; Jorgensen, P.; Hättig, C. *Int. J. Quantum Chem.* **1998**, *68*, 1–52.
(38) Olsen, J.; Jørgensen, P.; Helgaker, T.; Oddershede, J. *J. Phys. Chem. A* **2005**, *109*, 11618–11628.
(39) Takimoto, Y.; Isborn, C. M.; Eichinger, B. E.; Rehr, J. J.; Robinson, B. H. *J. Phys. Chem. C* **2008**, *112*(21), 8016–8021.
(40) Willets, A.; Rice, J. E.; Burland, D. M.; Shelton, D. P. *J. Chem. Phys.* **1992**, *97*, 7590–7600.
(41) Shi, R. F.; Garito, A. F. Introduction: conventions and standards for nonlinear optical processes. In *Characterization Techniques and Tabulations for Organic Nonlinear Optical Materials*; Kuzyk, M. G., Dirk, C. W., Eds.; Marcel Dekker: New York, 1998; Vol. *60*; p 1.
(42) Meyers, F.; Marder, S. R.; Pierce, B. M.; Bredas, J. L. *J. Am. Chem. Soc.* **1994**, *116*(23), 10703–10714.
(43) Beljonne, D.; Cornil, J.; Shuai, Z.; Bredas, J. L.; Rohlfing, F.; Bradley, D. D. C.; Torruellas, W. E.; Ricci, V.; Stegeman, G. I. *Phys. Rev. B: Condens. Matter* **1997**, *55*, 1505–1516.
(44) Di Bella, S.; Ratner, M. A.; Marks, T. J. *J. Am. Chem. Soc.* **1992**, *114*, 5842–5849.
(45) Priyadarshy, S.; Therien, M. J.; Beratan, D. N. *J. Am. Chem. Soc.* **1996**, *118*, 1504.
(46) Marder, S. R.; Gorman, C. B.; Meyers, F.; Perry, J. W.; Bourhill, G.; Bredas, J. L.; Pierce, B. M. *Science* **1994**, *265*, 632–635.
(47) Sim, F.; Chin, S.; Dupuis, M.; Rice, J. E. *J. Phys. Chem.* **1993**, *97*(6), 1158–1163.
(48) Tripathy, K.; Moreno, J. P.; Kuzyk, M. G.; Coe, B. J.; Clays, K.; Kelley, A. M. *J. Chem. Phys.* **2004**, *121*(16), 7932–7945.
(49) Isborn, C. M.; Leclercq, A.; Vila, F. D.; Dalton, L. R.; Bredas, J.-L.; Eichinger, B. E.; Robinson, B. H. *J. Phys. Chem. A* **2007**, *111*(7), 1319–1327.

(50) Jacquemin, D.; André, J.-M.; Perpète, E. A. *J. Chem. Phys.* **2004**, *121* (9), 4389–4396.
(51) Suponitsky, K. Y.; Liao, Y.; Masunov, A. E. *J. Phys. Chem. A* **2009**, *113*, 10994–11001.
(52) Dykstra, C. E.; Jasien, P. G. *Chem. Phys. Lett.* **1984**, *109*(4), 388–393.
(53) Hurst, G. J. B.; Dupuis, M.; Clementi, E. *J. Chem. Phys.* **1988**, *89*(1), 385–396.
(54) Rice, J. E.; Amos, R. D.; Colwell, S. M.; Handy, N. C.; Sanz, J. *J. Chem. Phys.* **1990**, *93*, 8828–8840.
(55) Fitzgerald, G.; Andzelm, J. *J. Phys. Chem.* **1991**, *95*(26), 10531–10534.
(56) Scheiner, A. C.; Baker, J.; Andzelm, J. *J. Comput. Chem.* **1997**, *18*(6), 775–795.
(57) Champagne, B.; Perpete, E. A.; Jacquemin, D.; van Gisbergen, S. J. A.; Baerends, E.-J.; Soubra-Ghaouri, C.; Robins, K. A.; Kirtman, B. *J. Phys. Chem. A* **2000**, *104*(20), 4755–4763.
(58) Perpete, E. A.; Jacquemin, D. *Int. J. Quantum Chem.* **2007**, *107*(11), 2066–2074.
(59) Runge, E.; Gross, E. K. U. *Phys. Rev. Lett.* **1984**, *52*(12), 997–1000.
(60) Furche, F. *J. Chem. Phys.* **2001**, *114*(14), 5982–5993.
(61) Furche, F.; Ahlrichs, R. *J. Chem. Phys.* **2002**, *117*(16), 7433–7448.
(62) Liang, W.; Isborn, C. M.; Lindsay, A.; Li, X.; Smith, S. M.; Levis, R. J. *J. Phys. Chem. A* **2010**, *114*(21), 6201–6206.
(63) Geskin, V. W.; Lambert, C.; Bredas, J. L. *J. Am. Chem. Soc.* **2003**, *125* (50), 15651–15658.
(64) Luo, Y.; Norman, P.; Rudd, K.; Agren, H. *Chem. Phys. Lett.* **1998**, *285*, 160–163.
(65) Tretiak, S.; Chernyak, V.; Mukamel, S. *Chem. Phys. Lett.* **1998**, *287* (1,2), 75–82.
(66) Dalton, L. R.; Harper, A. W.; Robinson, B. H. *Proc. Natl. Acad. Sci. U.S.A.* **1997**, *94*, 4842–4847.
(67) Dalton, L. R.; Robinson, B. H.; Alex, K.-Y.; Jen, A. K.-Y.; Steier, W. H.; Nielsen, R. *Opt. Mater.* **2003**, *21*, 19–28.
(68) Nielsen, R. D.; Rommel, H. L.; Robinson, B. H. *J. Phys. Chem. B* **2004**, *108* (25), 8659−8667; Nielsen, R. D. unpublished results
(69) Kim, W.-K.; Hayden, L. M. Fully atomistic modeling of an electric field poled guest-host nonlinear optical polymer. *J. Chem. Phys.* **1999**, *111*, 5212–5222.
(70) Leahy-Hoppa, M. R.; French, J.; Cunningham, P. D.; Hayden, L. M. Atomistic molecular modeling of electric field poling of nonlinear optical polymers. In *Nonlinear Optical Properties of Matter: Form Molecules to Condensed Phases*; Papadopoulos, M. G., Leszczynski, J., Sadlej, A. J., Eds.; Kluwer Press: New York, 2006; pp 337−357.
(71) Leahy-Hoppa, M. R.; Cunningham, P. D.; French, J. A.; Hayden, L. M. *J. Phys. Chem. A* **2006**, *110*, 5792–5797.
(72) Makowska-Janusik, M.; Reis, H.; Papadopoulos, M. G. *J. Phys. Chem. B* **2004**, *108*(2), 588–596.
(73) Robinson, B. H.; Dalton, L. R. *J. Phys. Chem A.* **2000**, *104*(20), 4785–4795.
(74) Rommel, H. L.; Robinson, B. H. *J. Phys. Chem. C* **2007**, *111*(50), 18765–18777.
(75) Johnson, L. E.; Barnes, R.; Draxler, T. W.; Eichinger, B. E.; Robinson, B. H. *J. Phys. Chem. B* **2010**, *114*(25), 8431–8440.
(76) Grote, J. G.; Dalton, L. R.; Sullivan, P; Robinson, B. H.; Eichinger, B. E.; Jen, A. K.-Y.; Benight, S.; Kosilkin, I.; Bale, D. H. *Nonlinear Opt., Quantum Opt.* **2010**, *40*, 15–26.
(77) Hammond, S. R.; Clot, O.; Firestone, K. A.; Bale, D. H.; Haller, M. H.; Phelan, G. D.; Carlson, B.; Jen, A. K.-Y.; Reid, P. J.; Dalton, L. R. *Chem. Mater.* **2008**, *20*(10), 3425–3434.
(78) Firestone, K. A.; Lao, D. B.; Casmier, D. M.; Clot, O.; Dalton, L. R.; Reid, P. J. *Proc. SPIE−Int. Soc. Opt. Eng.* **2005**, *5935*, 59350P1–5935P9.
(79) Smith, G. J.; Middleton, A. P.; Clarke, D. J.; Teshome, A.; Kay, A. J.; Bhuiyan, M. D. H.; Asselberghs, I.; Clays, K. *Opt. Mater.* **2010**, *32*, 1237–1243.
(80) Campo, J.; Desmet, F.; Wenseleers, W.; Goovaerts, E. *Opt. Express* **2009**, *17*(6), 4587–4604.
(81) Teng, C.; Man, H. *Appl. Phys. Lett.* **1990**, *56*, 1734–1736.
(82) Davies, J. A.; Elangovan, A.; Sullivan, P. A.; Olbricht, B. C.; Bale, D. H.; Ewy, T. R.; Isborn, C. M.; Eichinger, B. E.; Robinson, B. H.; Reid, P. J.; Li, X.; Dalton, L. R. *J. Am. Chem. Soc.* **2008**, *130*(32), 10565–10575.
(83) Park, D. H.; Lee, C. H.; Herman, W. N. *Opt. Express* **2006**, *14*(19), 8866–8884.
(84) Graf, H. M.; Zobel, O.; East, A. J.; Haarer, D. *J. Appl. Phys.* **1994**, *75* (7), 3335–3340.
(85) Olbricht, B. C.; Sullivan, P. A.; Davies, J. A.; Dennis, P. C.; Hurst, J. T.; Johnson, L. E.; Bale, D. H.; Benight, S. J.; Hilfiker, J. N.; Chen, A.; Eichinger, B. E.; Reid, P. J.; Dalton, L. R.; Robinson, B. H. *J. Phys. Chem. B* **2010**, submitted.
(86) Mansuripur, M. *J. Appl. Phys.* **1990**, *67*(10), 6466–6476.
(87) Woollam, J. A. In *Optical Metrology*; SPIE: Bellingham, WA, 1999; Vol. *CR72*; p 3.
(88) Johs, B. Overview of Variable Angle Spectroscopic Ellipsometry (VASE), Part II: Advanced Applications. In *Optical Metrology*; SPIE: Bellingham, WA, 1999; Vol. *CR72*; p 29.
(89) Gray, T.; Kim, T.-D.; Knorr, D. B., Jr.; Luo, J.; Jen, A. K.-Y.; Overney, R. M. *Nano Lett.* **2008**, *8*(2), 754–759.
(90) Knorr, D. B., Jr.; Zhou, X.-H.; Shi, Z.; Luo, J.; Jang, S.-H.; Jen, A. K.-Y.; Overney, R. M. *J. Phys. Chem. B* **2009**, *113*(43), 14180–14188.
(91) Gray, T.; Kilgore, J. P.; Luo, J.; Jen, A. K.-Y.; Overney, R. M. *Nanotechnology* **2007**, *18*, 044009−1–9.
(92) Knorr, D. B., Jr.; Gray, T. O.; Overney, R. M. *Ultramicroscopy* **2009**, *109*(8), 991–1000.
(93) Knorr, D. B., Jr.; Benight, S. J. Unpublished data for the C1 and related dendrimer systems.
(94) Huang, S.; Kim, T.-D.; Luo, J.; Hau, S. K.; Shi, Z.; Zhou, X.-H.; Yip, H.-L.; Jen, A. K.-Y. *Appl. Phys. Lett.* **2010**, *96*, 243311−1–3.
(95) Mao, S. S. H.; Ra, Y.; Guo, L.; Zhang, C.; Dalton, L. R.; Chen, A.; Garner, S. M.; Steier, W. H. *Chem. Mater.* **1998**, *10*, 146–155.
(96) Iacono, S. T.; Budy, S. M.; Jin, J.; Smith, D. W., Jr. *J. Polym. Sci., Part 1: Polym. Chem.* **2007**, *45*, 5706–5721.
(97) Budy, S. M.; Suresh, S.; Spraul, B. K.; Smith, D. W. *J. Phys. Chem. C* **2008**, *112*, 8089–8104.
(98) Ma, H.; Liu, S.; Suresh, S.; Liu, L.; Kang, S. H.; Haller, M.; Sassa, T.; Dalton, L. R.; Jen, A. K.-Y. *Adv. Funct. Mater.* **2002**, *12*(9), 565–574.
(99) Luo, J.; Haller, M.; Li, H.; Kim, T.-D.; Jen, A. K.-Y. *Adv. Mater.* **2003**, *15*(19), 1635–1638.
(100) Sullivan, P. A.; Olbricht, B. C.; Akelaitis, A. J. P.; Mistry, A. A.; Liao, Y.; Dalton, L. R. *J. Mater. Chem.* **2007**, *17*, 2899–2903.
(101) Dalton, L. R.; Sullivan, P. A.; Bale, D. H.; Olbricht, B. C. *Solid-State Electron.* **2007**, *51*, 1263–1277.
(102) Shi, Z.; Luo, J.; Huang, S.; Zhou, X. H.; Kim, T.-D.; Cheng, Y.-J.; Polishak, B. M.; Younkin, T. R.; Block, B. A.; Jen, A. K.-Y. *Chem. Mater.* **2008**, *20*, 6372–6377.
(103) Shi, Z.; Luo, J.; Hunag, S.; Cheng, Y.; Kim, T.; Polishak, B. M.; Zhou, X.; Tian, Y.; Jang, S.; Knorr, D. B., Jr.; Overney, R. M.; Younkin, T. R.; Jen, A. K.-Y. *Macromolecules* **2009**, *42*, 2438–2445.
(104) Shi, Z.; Hau, S.; Luo, J.; Kim, T.; Tucker, N. M.; Ka, J.; Sun, H.; Pyajt, A.; Dalton, L. R.; Chen, A.; Jen, A. K.-Y. *Adv. Funct. Mater.* **2007**, *17* (14), 2557–2563.
(105) Takahaskhi, S.; Bhola, B.; Yick, A.; Steier, W.; Luo, J.; Jen, A. K.-Y.; Jin, D.; Dinu, R. *J. Lightwave Technol.* **2010**, *27*(8), 1045–1050.
(106) Dinu, R.; Jin, D.; Yu, G.; Chen, B.; Huang, D.; Chen, H.; Barklund, A.; Miller, E.; Wei, C.; Vernagiri, J. *J. Lightwave Technol.* **2009**, *27*(11), 1527–1532.
(107) http://products.gigoptix.com/polymer_modulators
(108) Huang, Y.; Paloczi, G. T.; Yariv, A.; Zhang, C.; Dalton, L. R. *J. Phys. Chem. B* **2004**, *108*, 8606–8613.
(109) Song, H.-C.; Oh, M.-C.; Ahn, S.-W.; Steier, W. H. *Appl. Phys. Lett.* **2003**, *82*, 4431–4434.
(110) Chen, D.; Fetterman, H. R.; Chen, A.; Steier, W. H.; Dalton, L. R.; Wang, W.; Shi, Y. *Appl. Phys. Lett.* **1997**, *70*, 3335–3337.
(111) Lee, M.; Katz, H. E.; Erben, C.; Gill, D. M.; Gopalan, P.; Heber, J. D.; McGree, D. J. *Science* **2002**, *298*, 1401–1403.
(112) Wulbern, J. H.; Petrov, A.; Eich, M. *Opt. Express* **2009**, *17*(1), 304–313.
(113) Eich, M.; Wuelbern, J.; Hampe, J.; Petrov, A.; Luo, J.; Jen, A. K.; di Falco, A.; Krauss, T. F.; Bruns, J. *Proc. SPIE* **2009**, *7413*, 7413051−1–7.
(114) Block, B.; Younkin, T.; Davids, P.; Reshotko, M.; Chang, P.; Polishak, B.; Huang, S.; Luo, J.; Jen, A. K.-Y. *Opt. Express* **2008**, *16*(22), 18326–18333.
(115) Gan, H.; Greenlee, C.; Sheng, C.; Norwood, R. A.; Fallahi, M.; Wang, S.; Lin, W.; Yamanoto, M.; Mohanalingam, K.; Peyghambarian, N. *Appl. Phys. Lett.* **2008**, *92*, 203302−1–3.
(116) Bortnik, B.; Hung, Y.-C.; Tazawa, H.; Seo, B.-J.; Luo, J.; Jen, A. K.-Y.; Steier, W. H.; Fetterman, H. R. *IEEE J. Sel. Top. Quant. Electron* **2007**, *13*(1), 104–110.
(117) Zhang, C.; Dalton, L. R.; Oh, M.-C.; Zhang, H.; Steier, W. H. *Chem. Mater.* **2001**, *13*, 3043–3050.
(118) Cheng, Y.-J.; Luo, J.; Huang, S.; Zhou, X.; Shi, Z.; Kim, T.-D.; Bale, D. H.; Takahashi, S.; Yick, A.; Polishak, B. M.; Jang, S.-H.; Dalton, L. R.; Reid, P. J.; Steier, W. H.; Jen, A. K.-Y. *Chem. Mater.* **2008**, *20*, 5047–5054.
(119) Cheng, Y.-J.; Luo, J.; Huang, S.; Zhou, X.-H.; Shi, Z.; Kim, T.-D.; Bale, D. H.; Takahashi, S.; Yick, A.; Polishak, B. M.; Jang, S.-H.; Dalton, L. R.; Reid, P. J.; Steier, W. H.; Jen, A. K.-Y. *Chem. Mater.* **2008**, *20*(15), 5047–5054.
(120) Kuzyk, M. G. Physical Limits on Electronic Nonlinear Molecular Susceptibilities. *Phys. Rev. Lett.* **2000**, *85*(6), 1218–1221.
(121) Kuzyk, M. G. *Phys. Rev. Lett.* **2003**, *90*(3), 039902–1.
(122) Kang, H.; Facchetti, A.; Zhu, P.; Jiang, H.; Yang, Y.; Cariati, E.; Righetto, S.; Ugo, R.; Liu, Z.; Ho, S.; Marks, T. J. *Angew. Chem., Int. Ed.* **2005**, *44*, 7922–7925.
(123) Kang, H.; Facchetti, A.; Jiang, H.; Cariati, E.; Righetto, S.; Ugo, R.; Zuccaccia, C.; Macchioni, A.; Stern, C. L.; Liu, Z.; Ho, S.-T.; Brown, E. C.; Ratner, M. A.; Marks, T. J. *J. Am. Chem. Soc.* **2007**, *129*, 3267–3286.
(124) Brown, E. C.; Marks, T. J.; Ratner, M. A. *J. Phys. Chem. B* **2008**, *112*, 44–50.
(125) Wang, Y.; Frattarelli, D.; Facchetti, A.; Cariati, E.; Tordin, E.; Ugo, R.; Zuccaccia, C.; Macchioni, A.; Wegener, S. L.; Stern, C. L.; Ratner, M. A.; Marks, T. J. *J. Phys. Chem. C* **2008**, *112*, 8005–8015.
(126) Isborn, C. M.; Davidson, E. R.; Robinson, B. H. *J. Phys. Chem. A* **2006**, *110*(22), 7189–7196.
(127) Blanchard-Desce, M.; Baudin, J.-B.; Jullien, L.; Lorne, R.; Ruel, O.; Brasselet, S.; Zyss, J. *Opt. Mater.* **1999**, *12*, 333–338.

(128) Ray, P. C.; Leszcynski, J. *Chem. Phys. Lett*. **2004**, *399*, 162–166.
(129) Akdas-Kilig, H.; Roisnel, T.; Ledoux, I.; Le Bozec, H. *New J. Chem*. **2009**, *33*, 1470–1473.
(130) Valore, A.; Cariati, E.; Righetto, S.; Roberto, D.; Tessore, F.; Ugo, R.; Fragala, I. L.; Fragala, M. E.; Malandrino, G.; De Angelis, F.; Belpassi, L.; Ledoux-Rak, I.; Hoang Thi, K.; Zyss, J. *J. Am. Chem. Soc*. **2010**, *132*, 4966–4970.
(131) Quintiliani, M.; Pérez-Moreno, J.; Asselberghs, I.; Vázquez, P.; Clays, K.; Torres, T. *J. Phys. Chem. B* **2010**, *114*, 6309–6315.
(132) Huang, S.; Kim, T.-D.; Luo, J.; Hau, S. K.; Shi, Z.; Zhou, X.-H.; Yip, H.-Y.; Jen, A. K.-Y. *Appl. Phys. Lett*. **2010**, *96*, 243311−1–3.
(133) Fachetti, A.; Abbotto, A.; Beverina, L.; van der Boom, M. E.; Dutta, P.; Evmenenko, G.; Pagani, G. A.; Marks, T. J. *Chem. Mater*. **2003**, *15*, 33–38.
(134) Facchetti, A.; Annoni, E.; Beverina, L.; Morone, M.; Zhu, P.; Marks, T. J.; Pagani, G. A. *Nat. Mater*. **2004**, *3*, 910–917.
(135) Frattarelli, D.; Schiavo, M.; Facchetti, A.; Ratner, M. A.; Marks, T. J. *J. Am. Chem. Soc*. **2009**, *131*, 12595–12612.
(136) Kang, H.; Zhu, P.; Yang, Y.; Facchetti, A.; Marks, T. J. *J. Am. Chem. Soc*. **2004**, *126*, 15974–15975.
(137) Halter, M.; Liao, Y.; Plocinik, R. M.; Coffey, D. C.; Bhattacharjee, S.; Mazur, U.; Simpson, G. J.; Robinson, B. H.; Keller, S. L. *Chem. Mater*. **2008**, *20*, 1778–1787.
(138) Kwon, O. P.; Ruiz, B.; Choubey, A.; Mutter, L.; Schneider, A.; Jazbinsek, M.; Gramlich, V.; Gunter, P. *Chem. Mater*. **2006**, *18*, 4049–4054.
(139) Kwon, S.-J.; Hunziker, C.; Kwon, O.-P.; Jazbinsek, M.; Gunter, P. *Cyrst. Growth & Design* **2009**, *9*(5), 2512–2516.
(140) Kwon, S.-J.; Kwon, O.-P.; Jazbinsek, M.; Gramlich, V.; Günter, P. *Chem. Commun*. **2006**, *35*, 3729–3731.
(141) Khan, R. U. A.; Kwon, O.-P.; Tapponnier, A.; Rashid, A. N.; Günter, P. *Adv. Funct. Mater*. **2006**, *16*, 180–188.
(142) Hunziker, C.; Kwon, S.-J.; Figi, H.; Juvalta, F.; Kwon, O.-P.; Jazbinsek, M.; Günter, P. *J. Opt. Soc. Am. B* **2008**, *25*(10), 1678–1683.
(143) Figi, H; Mutter, L.; Hunziker, C.; Jazbinšek, M.; Günter, P.; Coe, B. J. *J. Opt. Soc. Am. B* **2008**, *25*(11), 1786.
(144) Kwon, S.-J.; Jazbinsek, M.; Kwon, O.-P.; Gunter, P. *Cryst. Growth Des*. **2010**, *10*, 1552–1558.
(145) Cox, C. H., III; Ackerman, E. L. *J. Phys. Chem. B* **2004**, *108*(25), 8540–8542.
(146) Lin, C.-Y.; Wang, X.; Chakravarty, S.; Lee, B. S.; Lai, W.; Luo, J.; Jen, A. K.-Y.; Chen, R. T. *Appl. Phys. Lett*. **2010**, *97*, 093304−1–3.